Snezana Radivojev, MSc

Characterization of potential new dry powder inhaler formulations

MASTER'S THESIS

to achieve the university degree

of Master of Science

Master's degree programme: Chemical and Pharmaceutical Engineering

submitted to

Graz University of Technology

Supervisor

Univ.-Prof. DI Dr. Johannes Khinast

Research Center Pharmaceutical Engineering GmbH

Dr. Sarah Zellnitz
Research Center Pharmaceutical Engineering GmbH

Graz, April 2017

AFFIDAVIT

I declare that I have authored this thesis independently, that I have not used other than the declared sources/resources, and that I have explicitly indicated all material which has been quoted either literally or by content from the sources used. The text document uploaded to TUGRAZonline is identical to the present master‘s thesis.

Date	Signature

Acknowledgment

Firstly, I would like to thank and express my sincere gratitude to my supervisors Johannes Khinast, Sarah Zellnitz and Joana Pinto. Dear Sarah, I highly appreciate your patience, guidance, motivation and support throughout my work.

A huge thanks goes to you Joana for your insight, help, discussions and knowledge sharing. The quality, outcome of this work and personal progress would not be the same without you.

Furthermore, I am thankful to Amrit Paudel, Philipp Pernitsch and the rest of the RCPE team for their technical support.

I would like to dedicate this thesis to my family, my parents Milan and Sonja, my sister Natasa, my partner Valon and my ‘‘sister’’ Carolina and ‘‘brother’’ Ian, as well as to all my friends. Without your advice, understanding, tears and joy I would not be here where I am now. You trust and believed in me and for that, I am forever grateful.

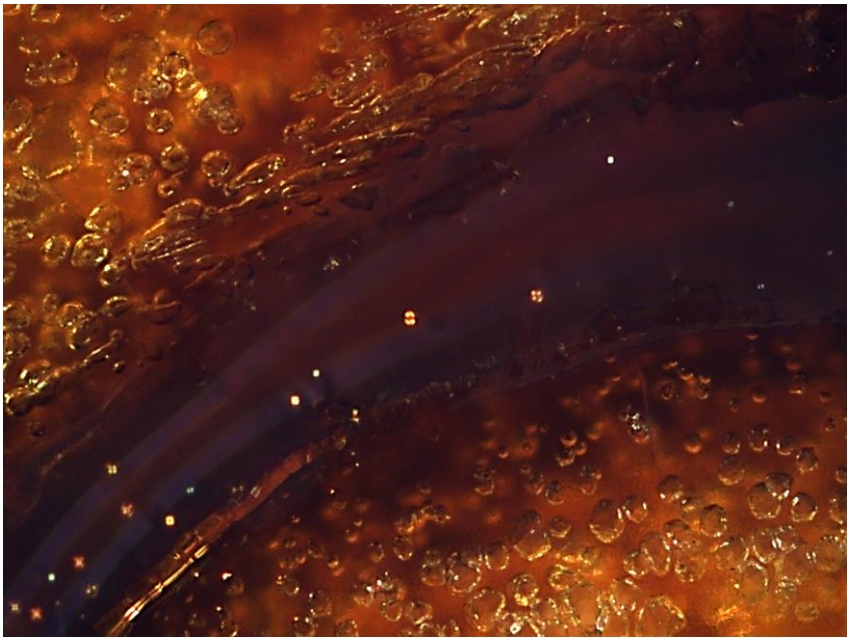

‘‘I was taught that the way of progress was neither swift nor easy’’

Contents

Abstract

Inhaled medications attract attention during the last decades due to various advantages such as higher bioavailability, smaller drug concentration needed due to the avoidance of the first pass effect, simplicity and a wide spectrum of applicable active pharmaceutical ingredients (APIs). The type of formulations investigated in the present study are carrier-based formulations where the API particles (1-5 µm) are blended with larger excipient carrier particles to improve stability and flowability of the formulation. During inhalation, the API has to be detached from the carrier, as only particles of 1-5µm are able to reach the lung. In order to generate particles of the inhalable size secondary processing like jet milling or spray drying is usually applied. Nevertheless, these processes may influence properties of the resulting particles like the solid-state, shape, surface energetics and the stability, which in turn can affect the quality, and performance of inhalable formulations.

Therefore, the aim of this work was to evaluate the impact of secondary processing on salbutamol sulphate properties. Spray dried as well as jet milled salbutamol sulphate particles were characterized by Small and Wide Angle X-ray scattering (SWAXS), Fourier Transform Infrared Spectroscopy (FTIR), Differential Scanning Calorimetry (DSC) and optical microscopy while surface energetics were determined via the contact angle method. After secondary processing, the differently produced API particles were blended with a model carrier, and the DPI formulations were characterized via scanning electron microscopy (SEM) and Next Generation Impactor (NGI). Further, the stability of both API particles and mixtures were studied for 21 days, with particular focus on the change of the API solid-state under elevated humidity.

This study showed that secondary processing significantly affects particle shape and solid state and that particles generated via spray drying are more susceptible to changes due to elevated storage conditions. Concerning the aerodynamic performance, the results show that milled, needle-like shaped, largely crystalline particles show better lung deposition when compared to spray dried, spherical, predominately amorphous particles.

Abstrakt

Die inhalative Therapie erlangt immer mehr Bedeutung aufgrund zahlreicher Vorteile, wie eine erhöhte lokale Bioverfügbarkeit, die geringe Wirkstoffmenge die verabreicht werden muss da der First-pass Effekt umgangen wird, die einfache Anwendung und die Vielfalt der Wirkstoffe die mittels diesem Weg verabreicht werden kann. Die vorgelegte Arbeit beschäftigt sich mit trägerbasierten Formulierungen bei denen die Wirkstoffpartikel (1-5µm) mit größeren Trägerpartikeln gemischt werden um die Stabilität und Fließfähigkeit der Formulierung zu erhöhen. Während des Inhalationsvorganges muss sich der Wirkstoff jedoch wieder vom Träger lösen um seinen Wirkort, die Lunge zu erreichen. Um Partikel in einer Größenordnung geeignet für die Inhalation herzustellen werden unterschiedliche Bearbeitungstechniken wie Mahlung/Mikronisierung oder Sprühtrocknung eingesetzt. Diese Herstellungsprozesse jedoch können die Partikeleigenschaften, wie Festkörpereigenschaften, Größe, Form und Stabilität, verändern, welche sich im Gegenzug auf die Qualität der Formulierung auswirken können.

Demnach ist das Ziel dieser Arbeit die Untersuchung des Einflusses von unterschiedlichen Bearbeitungstechniken auf die Partikeleigenschaften von Salbutamol Sulfat als Modelwirkstoff. Dazu wurden sprühgetrocknete so wie gemahlenen Slabutamol Partikel mittels Röntgenbeugung Fourier Transformation Infrarot Spektroskopie (FTIR), Dynamischer Differenzkalorimetrie und optischer Mikroskopie untersucht. Zusätzlich wurde die Oberflächenenergie über die Kontaktwinkelmethode ermittelt. Nach der Bearbeitung wurden die unterschiedlich prozessierten Wirkstoffpartikel mit einem Modellträger gemischt und die resultierenden Formulierungen mittels Rasterelektronenmikroskoie (REM) und dem Next Generation Impactor (NGI) untersucht. Darüber hinaus wurde die Stabilität der unterschiedlich hergestellten Wirkstoffpartikel und der Mischungen, mit speziellem Fokus auf feuchteinduzierte Festkörperänderungen der Wirkstoffpartikel, über einen Zeitraum von 21 Tagen studiert.

Die vorgelegte Studie hat gezeigt, dass sich die Bearbeitungstechnik deutlich auf die Partikelgröße, die Partikelform und den Festkörperzustand auswirkt und dass

sprühgetrocknete Salbutamol Partikel anfälliger sind für feuchteinduzierte Änderungen während der Lagerung. Bezüglich Inhalationseigenschaften konnte gezeigt werden, dass gemahlene, nadelförmige und Großteils kristalline Salbutamol Partikel eine bessere Lungengängigkeit erzielen, im Verglichen mit sprühgetrockneten runden, vorwiegend amorphen Partikeln

1. Introduction

1.1. Pulmonary drug delivery

Over the years, inhaled medication has been widely accepted for treating various respiratory diseases like asthma or chronically obstructive pulmonary disease. Besides local therapy, this route of administration was also investigated for systemic therapy.

Pulmonary drug delivery has several advantages. It allows avoiding the first-pass metabolism in the liver and possible poor gastrointestinal absorption. Moreover, a therapeutic effect can be achieved with less concentration of medication in comparison to systemic drug delivery [1, 2]. Deposition of active pharmaceutical ingredient (API) particle in the lung is achieved by different types of inhalers containing solid or liquid formulation. Liquid formulations are used in nebulizers and metered-dose inhalers (MDIs), while dry powder inhalers (DPIs) contain solid dosage form. Higher stability, the absence of propellants and simplicity of use make DPIs preferred delivery devices for inhalation therapy. However, the concentration of the drug that reaches the lung depends on the inspiration flow rate of the patient, which can be critical for dose uniformity [3].

Two types of dry powder inhaler formulations are known. The first include a system that consists of API or API and excipient agglomerates, resulting in carrier free DPIs. In order to be successfully deposited in the respiratory tract, the particle size of the API must be between 1-5μm (fine particles). Particles bigger than 5μm will be lost for lung deposition due to impaction in the throat and oral ingestion, while particles smaller than 1μm undergo Brownian motion and can be exhaled. This requirement is rather challenging because small particles are highly cohesive and have poor flowability due to high surface area to mass ratios. Therefore, the process of preparing carrier free formulations must be well controlled in order to establish loose API agglomerates. Overcoming this problem is possible by using the second approach, carrier based formulations. In carrier based formulations the API is adhered to the surface of a larger carrier. The size of carrier particles usually is between 50 and 200μm (coarse particles) and their

role is to improve powder flowability, reproducible dosing and aerosolization, the process where the API particles detach from the carrier [4, 5].

1.1.1. Available devices for pulmonary drug delivery

Besides the above mentioned parameters that might have a negative impact on the delivery of aerosols to the lung, the design of the device plays an important role in reproducibility of the dose and physicochemical stability of the drug [6].

Dry powder inhalers were developed as an approach to overcome limitations of nebulizers and MDIs. Currently, designs of DPIs include pre-metered or device metered systems in which the formulation is placed in either capsules, blisters, premetered discs and cartridges or reservoirs, respectively. Both of these designs can be used in single or multi dose systems.

This work focuses on single dose capsule DPIs. A capsule containing the drug formulation is placed into a holder inside of the device and opened within the device, by piercing the capsule followed by the inhalation of the powder. This concept was presented for the first time in the 1970s by Bell et al. A new capsule needs to be inserted into the device for each inhalation step. An example of this device is the Aerolizer (Figure 1) [7].

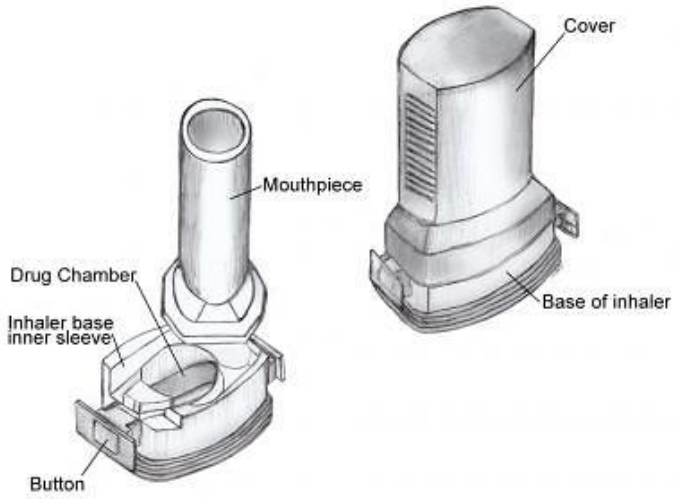

Figure 1: Aerolizer inner structure scheme [8]

Despite these devices have been on the market for a long time, the problem of low efficacy still remained a challenge [2]. A few factors have to be considered for the development of new DPIs:

a) properties of the formulation

b) generation of aerosol and delivery of the API

c) design of the device

d) correct inhalation technique and

e) the inspiratory flow rate.

The last two factors are particularly problematic for asthmatic infant patients or elderly patients because the required flow rates cannot be always achieved in passive devices [6, 7].

In pulmonary drug delivery, development of DPIs is accelerating rapidly, with innovations in every crucial aspect, from the design of the device to the formulation itself. Nevertheless, limitations still exist which is why these systems are a tempting field for constant improvement.

1.1.2. Evaluation of aerodynamic particle size distribution

Several parameters can be used in the characterization of DPIs such as aerodynamic particle size distribution (APSD), mass median aerodynamic diameter (MMAD) and fine particle fraction (FPF). APSD gives information on particle behavior in the air stream during inhalation. Furthermore, it allows an estimation of API deposition in the respiratory system together with MMAD [9]. FPF gives the percentage of particles below 5µm that are deposited in the lower airways related to all particles emitted from the device.

The aerodynamic diameter, d_A is described as the diameter of a sphere of unit density, which reaches the same velocity as a non-spherical particle in the air flow. This dimension depends on the particulate properties such as size, shape, density and airflow. An equation that can be used for estimation of d_A (Equation 1.) is derived from Stokes' law:

$$d_A = d_V \sqrt{\frac{\rho}{\rho_0 \chi}} \quad (1)$$

where d_V is the volume-equivalent diameter, ρ_0 is the unit density, ρ the particle density and χ the dynamic shape factor [10].

Instruments used in the evaluation of APSD and FPF are so called impactors in which the stream of the aerosol is executed through a series of stages. Every stage has a defined dimension described by the cut-off diameter. All particles larger than the stage's cut-off diameter will be held on that stage while the smaller particles will go with the air stream to the next one. If the air flow is known, the cut off diameter can be calculated with Equation 2:

$$D_{50Q} = D_{50Qn} \left(\frac{Q_n}{Q}\right)^{\frac{1}{2}} \quad (2)$$

where D_{50Q} is the cut-off diameter at the airflow rate Q_n=60L/min and Q is the airflow rate used during testing [3, 11].

In European and United States Pharmacopoeia a twin-stage impinger, Andersen Cascade Impactor (ACI), Marple-Miller impactor, Multi-Stage Liquid Impinger (MSLI) or Next Generation Impactor (NGI) are used for analyzing DPIs. Within this study, the NGI was used.

NGI is an assembly of an inhaler mouthpiece, preseparator, induction port and 8 collection stages (Figure 2). The flow control valve, solenoid valve, timer and vacuum pump are generally part of any impactor type. The role of the preseparator is to confiscate large carrier particles during testing of potential DPI formulation.

One necessary parameter during analysis is the pressure drop of 4kPa across the inhaler that needs to be achieved. Moreover, the airflow will influence cut-off points of each stage and has to be adapted to guarantee the required pressure drop. An airflow range between 30-100L/min is available for testing.

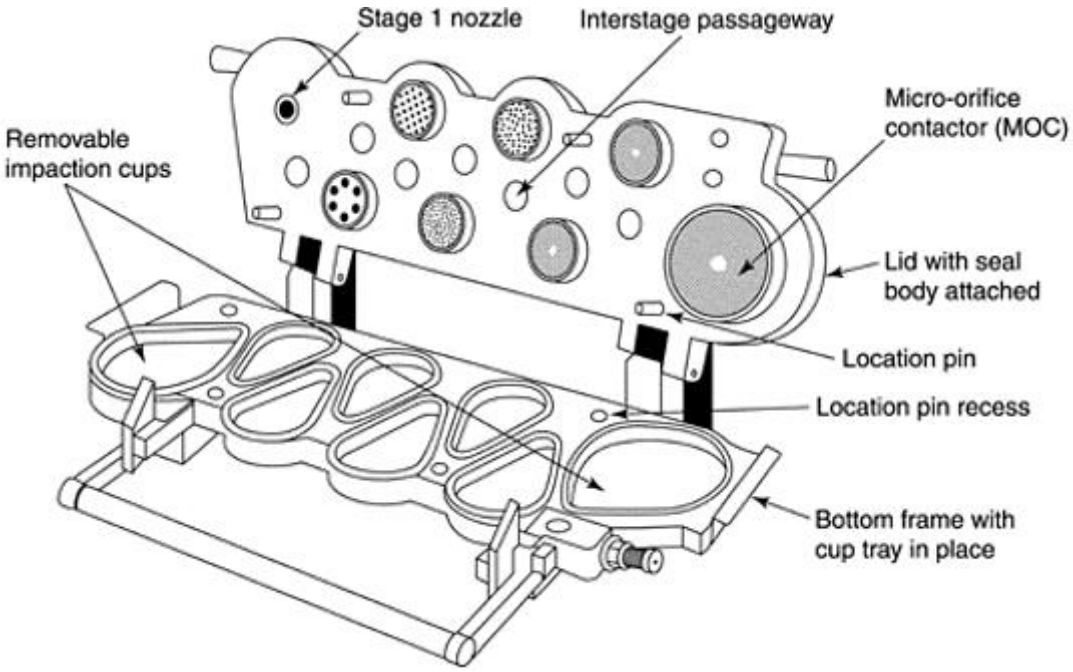

Figure 2: Next Generation Impactor scheme [12]

Although it is a time-consuming method, the NGI is a good tool to illustrate and mimic powder deposition in the lung [3].

1.2. Particle/powder properties

1.2.1. Solid-State

Remarkable efficiency of aerosols might be achieved by evolving optimized formulation. This implies that chemical and physical stability of the powder i.e. solid-state form must be well-known. Generally, particles can be crystalline or amorphous (Figure 3) [10].

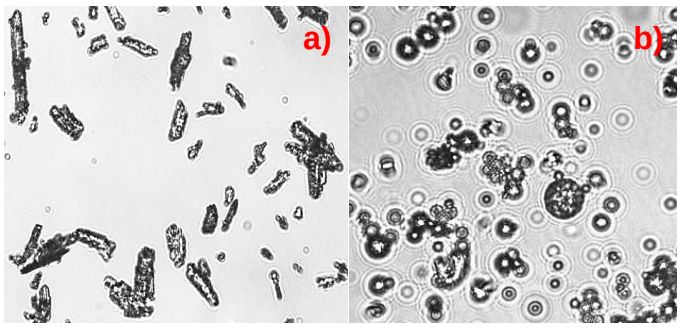

Figure 3: a) crystalline and b) amorphous salbutamol sulphate (SS)

In general, crystals are characterized by a long-range translational-orientational symmetry [13].

The crystalline form can be described by polymorphs or pseudopolymorphs. The ability of crystals to display some other lattice structures or molecular conformations without change in its chemical composition is a phenomenon known as polymorphism. Pseudopolymorphs are solvates and hydrates, crystals which bind water or some other molecules (organic solvents) to the crystal structure [14]. By contrast, amorphous solids do not have a long-range in molecular packing. Their advantages are a higher dissolution rate and solubility, but they have higher Gibbs free energy. Since they are less stable, both physically and chemically they can re-crystallize or undergo structural relaxation, changing the surface characteristics of the powder [15]. Kinetics of structural relaxation depends on environmental conditions such as temperature or humidity, which may influence the level of molecular mobility in the material [16].

Another possibility is the existence of disorder in crystalline materials. This means that during secondary processing, amorphous regions can appear in crystalline materials, which might be beneficial in some cases. This phenomenon is called mechanical activation, and it is rarely uniform to the powder and usually dominant on the surface [17]. Moreover, mechanical activation influences reactivity, conductivity, surface free energy and true density of the powder and these variations might influence the performance of the inhalation product [16].

Various methods are used in solid state characterization. The detection limit for quantification of amorphous content is 5-10% in most of the techniques, which can be problematic when small amorphous content exists on the surface of the powder [18]. The techniques used in this study will be explained in chapter 2.

1.2.2. Micrometrics

The determination of particulate properties is important for processes in different industries, such as the pharmaceutical, chemical, food industry etc. Special attention is given to particle size, shape, density and porosity.

Considering the necessary particle size of the API (1-5μm) for DPI formulations, the determination of particle size is of great interest. There are many variables

that are used for describing the size of regular particles, for example, Feret's or Martin's diameter, equivalent spheres diameter and so on. For the description of the particle population, however, the particle size distribution (PSD) is used. PSD can be represented by a cumulative or frequency curve and it can be based on number (q0, Q0), length (q1, Q1), area (q2, Q2) or mass/volume (q3, Q3) [19].

The shape of the particles has a great impact on the DPI aerosolization performance. Different shaped particles (spherical or needle-like) can be influenced by different terminal velocities and drag forces which affect the particles deposition in the respiratory tract [20]. The effect of particle shape has been widely investigated, showing contradictory results. In the review published by Kaialy it is, for instance, reported that adhesive mixtures containing more elongated carrier particles result in increased FPFs [21, 22]. Furthermore, needle-shaped crystals will have a higher ability to stay airborne in the airflow. These findings are in agreement with work published by Chow et al. [10]. However, this improvement has a certain limit because particles with higher elongation ratio might remain in the device or be deposited in the throat. An additional disadvantage is their poor flowability. According to Peng et al., spherical particles with low density have the ability to bind the API for a longer period, reducing the drug loss at low flow rates and thereby enhance the drug delivery [20].

Studies regarding the influence of the roughness of the carrier particles are rather conflicting. For example, Kawashima et al. reported that lactose carrier particles with increased surface roughness improved the FPF, while smoother spherical particles did not have a positive effect on the FPF [23]. Furthermore, Donovan and Smyth [24] showed that rough carrier particles improve the dispersion of the formulation, while Zeng et al. reported that smoothing the surface of the particles leads to higher FPF [25]. Stank and Steckel reported that dry particle coating can be used to improve the physical stability and dispersion of the powder mixture. They used glycerolmonostearate and magnesium stearate as excipients and concluded that increased dispersion might be the result of excipient deposition onto the API surface resulting in reduced surface roughness [26].

In purpose of this thesis, particle size distribution and shape of API were determined. Furthermore, a surface analysis of the adhesive mixtures was done. Methods will be discussed in chapter 2.

1.2.3. Surface energetics

Surface morphology coupled with particle size and shape have an impact on the surface energy of the powder. All of these factors need to be balanced in order to formulate stable DPI products. It is well known that surface energetics have a direct influence on interparticulate forces existing between the API and the carrier. Lower surface energy of the particles is favorable because it provides interparticulate forces to be strong, but low enough so that successful aerosolization can occur. Moreover, surface energetics of the API crystal surface might influence the type of chemical interactions with the carrier particles directly leading to reduced aerosolization and lower dose delivery. [14].

It is well reported that many methods may be employed in order to measure surface energy, e.g. the inverse gas chromatography (IGC) [16, 27], isothermal microcalorimetry [13, 28], atomic force microscope (AFM) and the contact angles method [13].

The contact angle method is widely used and results obtained using this method are comparable to results obtained when using other methods. This method measures the contact angle between liquid and solid samples. When assessing the surface free energy of the powder, compacted powder represents the solid sample and contact angles must be measured with several liquids. Measuring contact angles with homogenous surfaces leads to results of great accuracy. However, when using the compacted powder as a solid sample, one of the drawbacks is the irregular surface of the powder. The accuracy of this method may be reduced, because the powder may not always be compacted onto the surface properly, liquid may pass away through the pores, resulting in the penetration of loose agglomerates [13, 29].

From contact angles measurements, the surface free energy of the solid can be calculated using the Good and van Oss method in which the contact angle of three liquids is measured. The acid (γ^+), base (γ^-) and non-polar (γ^{LW}) components

of the solvent must be known. The surface free energy is calculated using equation 3:

$$(1 + cos\theta)\gamma_i{}^{tot} = 2(\sqrt{\gamma_s{}^{LW}\gamma_l{}^{LW}} + \sqrt{\gamma_s{}^{+}\gamma_l{}^{-}} + \sqrt{\gamma_s{}^{-}\gamma_l{}^{+}} \quad (3)$$

where the $\gamma_s{}^{LW}$ $\gamma_l{}^{LW}$ are non-polar components of tested solid and liquid and $\gamma_s{}^{+}$, $\gamma_s{}^{-}$, $\gamma_l{}^{+}$, $\gamma_l{}^{-}$ are polar components of tested solid and liquid, respectively, θ is the measured contact angle value between solid and liquid and $\gamma_i{}^{tot}$ is the surface tension of the tested liquid.

The resulting surface free energy represents the sum of non-polar (Lifshitz-van der Waals, LW) and polar (acid-base, AB) components. Following these calculations, there is a possibility for determination of the work of adhesion (W^{adh}, equation 4) and the work of cohesion (W^{coh}, equation 5) between the API and the carrier.

$$W_{ij}{}^{adh} = \gamma_i + \gamma_j - \gamma_{ij} \quad (4)$$

$$W_{ii}{}^{coh} = 2\gamma_{ii} \quad (5)$$

γ_i and γ_j are the surface energies of the tested interacting materials and γ_{ij} is the interfacial energy of their surfaces.

If three liquids are used, optimal combinations are water/glycerol/bromonaphthalene and water/glycerol/diiodomethane [29, 30].

The value of the contact angle can also be explained as a measure of competing cohesion energy of the liquid and the adhesion energy between liquid and solid.

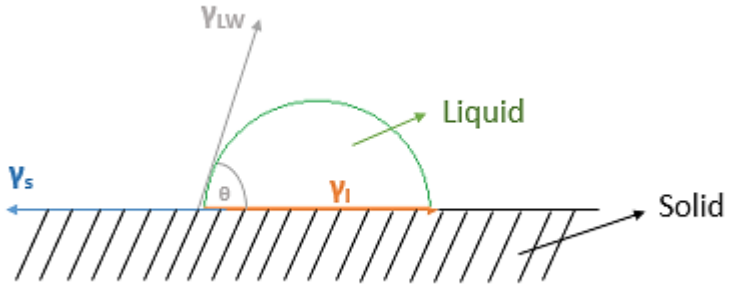

Figure 4: Schematic representation of the contact angle, adapted from [31]

Precise determination of powder surface energetics can improve DPI formulations. When values of surface free energy are known, it is possible to select combinations of different carriers and APIs in order to improve the aerosol performance.

1.2.4. Crucial factors influencing the aerosol deposition in the respiratory tract

The lung is a remarkably tempting target for drug delivery for many reasons, mainly because it provides an excessive surface area with small enzymatic activity. The anatomy of the respiratory tract plays a fundamental role in maintaining the optimal environment of the lung. At the same time, this represents a barrier for therapy efficacy leading to extensive research of different powder aerosols performance, including dry powder inhalers [1, 32].

Factors influencing the DPI performance are shown in Figure 5.

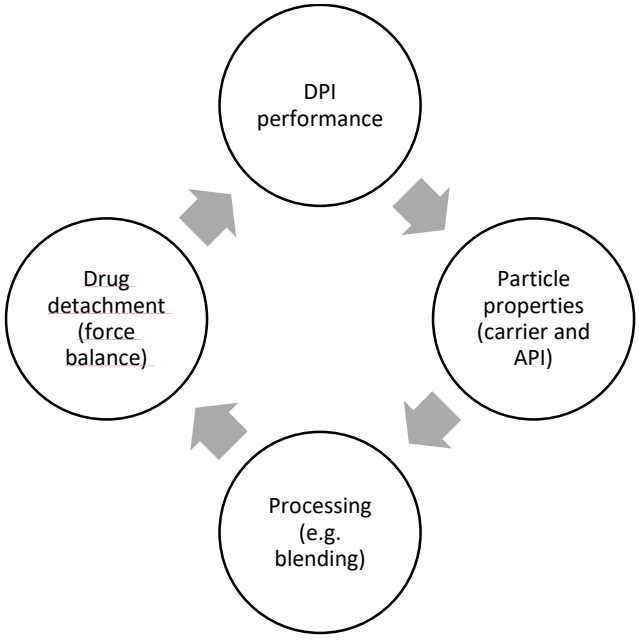

Figure 5: Relationship between different processes influencing DPI performance

Tightly connected to the DPIs performance is the aerosolization performance, which means the detachment of the API from the carrier particles, their dispersion in the air flow and finally the deposition in the respiratory tract. This process can

be influenced by particle size and shape of the components, the roughness of their surfaces, the existence of amorphous regions etc. These factors can be controlled by engineering the particles. Another influencing factor is powder processing, e.g. blending [4].

As mentioned before, the particle size (1-5μm) is the main requirement for successful deposition of the API. Small, fine particles are cohesive and have less flowability in comparison to coarse ones. The final formulation must have sufficient flowability in order to obtain reproducible dosing during the dispersion from the DPI device or during the process of automatic filling in the industry [33]. This problem can be solved in with two different ways:

a) by controlling aggregation of particles which will lead to the formation of loosely adherent floccules improving dispersion or

b) by using carrier based formulations which consist of fine API particles blended with coarse carrier particles.

Using the second approach has its challenges. The interaction between the drug and the carrier will have an important influence on the DPIs performance. Forces acting between carrier and API have to be well balanced in order to guarantee detachment during inhalation. Moreover, it is important to mention that interaction between API particles itself can be a source of poor detachment.

Particulate interactions in pharmaceutical powders can be separated into two main categories: adhesive and cohesive. Cohesive interaction exists between molecules of the same species and similar size, while adhesive forces occur between different powder molecules [4].

Adhesive and cohesive forces exist due to a combination of mechanical interlocking as a result of surface roughness, so-called capillary forces, which occur due to the presence of water in the powder, electrostatic and van der Waals forces arising from the nature of the material [14].

Cohesive and adhesive interactions need to be balanced, known as cohesive-adhesive balance (CAB). As already mentioned, adhesion forces should be strong enough to secure uniform dosage, but weak enough to allow detachment of the drug during aerosolization (Figure 6) [20].

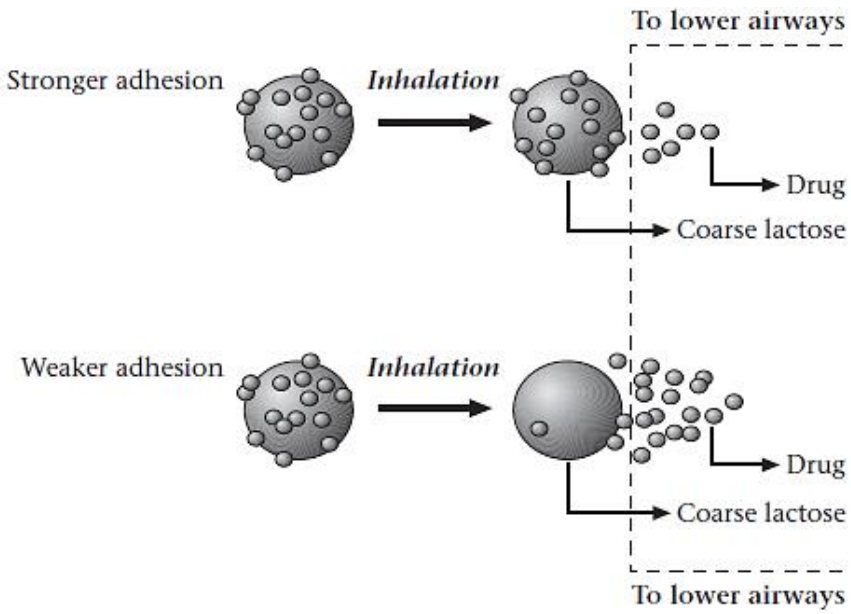

Figure 6: Influence of adhesion on the lung penetration [3]

The agglomeration of the API is one factor influencing the dose uniformity and the availability of API particles to the lower airways. In general, it can be explained as a process of forming bigger particles by sticking together primary particles. More precisely, agglomerates represent systems in which primary particles are held together by interparticulate forces. Agglomeration is usually an undesired consequence of small particle sizes and storage conditions linked to elevated temperature and moisture level.

The moisture level plays an important role in increasing the adhesion forces. An increased moisture level will directly increase the adhesion forces and particles will more or less randomly collide and form porous agglomerates. This process is known as ‘‘collision agglomeration’’ or ‘‘controlled growth agglomeration’’.

The link between the strength of agglomerates and their breakage is an important parameter in DPIs formulations. For instance, if agglomerates do not break, their size will be bigger than required for respiratory delivery, at the same time reducing the concentration of the API deposited in the lung [34]. Mechanical properties of particles or of the particle surface are crucial for the final strength of agglomerates. The strength of agglomerates can be increased by a phenomenon called sintering.

In general, sintering is a process where due to the high temperature primary particles form bigger, porous particles. There are several types of sintering (Figure 7). In solid-state sintering the driving force is the reduction of the surface free energy. This reduction is small, but the distance between particles is also rather small and occurs in samples not containing any liquid. In liquid-phase sintering the sample contains less than a few volume percent of the liquid. In some examples, the percentage of liquid is so small and difficult to detect so it can be interpreted as solid-state sintering. By increasing the moisture level and arising the temperature, particles will build viscous bridges between each other by viscous flow, resulting in viscous sintering, in which a consolidated mass of glassy particles will thicken, and lead to a greater strength of agglomerates [32, 35].

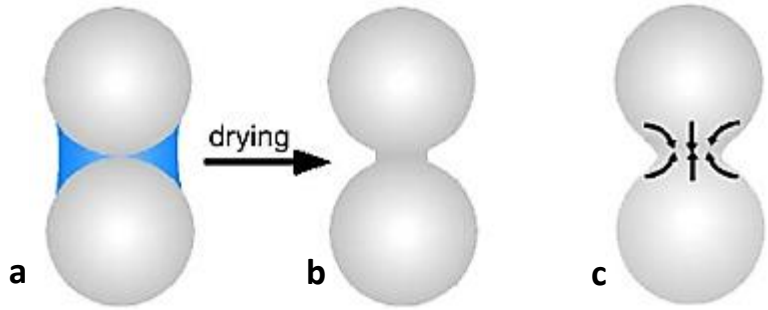

Figure 7: Adhesion principles a) liquid bridge, b) dried liquid bridge, c) sinter bridge; adapted from [32]

An additional influencing factor is de-agglomeration leading to improved performance. Understanding the magnitude of the agglomerate strength and the process of de-agglomeration is therefore of great importance as the performance level of DPIs depends on it [36].

1.3. Processing of raw materials

1.3.1. Milling techniques

Currently, marketed DPI formulations contain API particles which are processed (secondary processing) with one of the available methods in order to get inhalable size of particles. Besides size reduction other beneficial factors related to

secondary processing can be improved stability, deagglomeration and narrowing of the particle size distribution.

By the use of different milling techniques, the particle size is reduced due to friction, attrition, pressure, shear or impact. Proven methods are ball-milling, vibration milling and jet milling. As a result, generally crystalline, dense particles are produced with an irregular shape.

Jet-milling is a process in which the raw material endures many impact processes and smaller particles are separated by inertial impaction. Precisely, particles get reduced by collision of particles induced by high-pressure air or nitrogen fed through the nozzles. Flexible parameters are pressure and powder feed rate allowing the reduction of the size of the particles down to 1μm.

However, milling is a strong mechanical process which may alter the crystallinity of the particles. The main problem is the creation of amorphous regions during the process. Considering amorphous thermodynamic instability, it is logic to conclude that these regions will recrystallize. This will lead to the growth of crystals on the particle surface and sintering. Additionally, particles produced by milling have a high surface energy, which will increase the cohesion. Moreover, flat and small (needle-like) particles will have a large contact area which will increase adhesion.

Due to limited control of parameters, other techniques were developed in which particles are formed from solution, emulsions etc. [4, 10, 27, 37].

1.3.2. Spray Drying

Spray drying as a technique has been employed for many years and is widely used for the production of pharmaceutical particles. In a single step a solution is transformed into powder. Additionally, aside solution emulsions, suspensions or liposomes can be used as a feedstock. Atomization, drying and separation are the three main operations of the process (Figure 8).

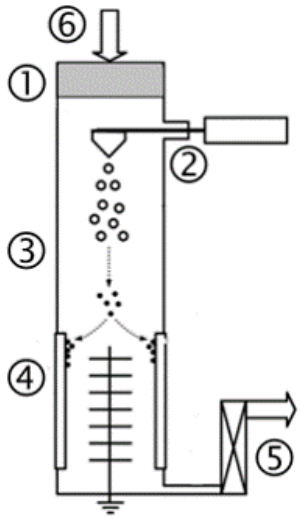

Figure 8: Schematic diagram of spray drying process 1) heating, 2) droplet formation, 3) drying chamber, 4) particle collection, 5) outlet filter, 6) drying gas [38]

Briefly, the feed is atomized to a spray, which is in immediate contact with hot air leading to a rapid evaporation of the spray droplets and to particle formation. The liquid is transformed into droplets in atomization. Methods of atomization are, for example, pneumatic, centrifugal or electrostatic atomization. Type of method coupled with the nozzle design determines the particle size distribution.

After atomization, the droplets are submitted to the drying process. Varying the inlet and outlet temperatures, the humidity of the gas used for the drying, the gas flow rate and the residence time will result in different end products. These parameters have a direct influence on size, shape, crystallinity, density and possible solvent residue. The humidity of the gas is crucial for forming agglomerates, considering that might increase capillary forces, forming the liquid bridges.

The particles produced are generally amorphous. Moreover, spray dried particles are spherical with less contact area and thus decreased cohesive and adhesive forces.

Compared to the milling processes, spray drying is a more controlled process that can produce particles for respiratory use [39]. Optimization of microscopic and macroscopic characteristics such as flowability, dispersibility and bulk density is possible. Interestingly many studies have shown that the FPF increases

with the use of spray dried particles. Lower surface energy is established with the use of this process and this might have an additional positive effect on deagglomeration. However, it is necessary to note that amorphous powders are not thermodynamically stable and understanding the behavior of the formulation due to storage and different environment is crucial [4, 10, 27, 37].

1.3.3. Blending

Blending is one of the crucial factors directly influencing the DPI performance. Generally, it can be defined as an energy consuming process in which two or more diverse portions of a material are displaced until homogeneity is achieved. In systems consisting of a drug and a carrier, blending involves breaking up the API agglomerates and the adhesion of API to the carrier particles.

The adhering process of fine API particles can be explained by two mechanisms:

a) fractionation of small API agglomerates due to their collision with carrier particles and blending vessel walls or
b) removing of API particles from broken agglomerates by erosion due to the intimate contact of agglomerates with carrier particles and blending vessel walls.

Compared to random mixtures, the possibility of segregation is minimized in adhesive mixtures, also reducing the demixing. This is because the attractive forces responsible for attaching the API to the carrier exceed the gravitational forces that try to separate them. During blending, three factors need to be balanced in order to successfully produce a stable formulation. The first one is the breaking up of already formed agglomerates in starting materials followed by the distribution of API to the carrier. The last one is the generation of forces that press the API to the carrier particles. These forces may radically increase the cohesive and adhesive forces.

The balance between these factors can be estimated via homogeneity of the blend. This parameter will depend on blending equipment (e.g. the mixer efficiency and blending conditions), solid state of the mixed particles and environmental factors (e.g. handling or relative humidity).

Blending conditions, i.e. blending time and speed, are the crucial factors in the preparation of adhesive mixtures. Increasing the blending time and speed can improve the homogeneity especially if there is great physico-chemical difference between mixed particles. However, the positive effect because of this increase is limited. Interactions between the API and the carrier will reach equilibrium at a certain point after which improvements are not possible [21].

1.3.4. Influence of different material properties on the stability and inhalation product performance

The basis for the development of DPI formulations is understanding particle behavior. This and the performance of aerosols is strongly linked to the physico-chemical characteristics of the powder [33].

The stability and bioavailability of particles are strongly dependent on the crystallinity of the material used. Methods that are used in particle engineering could alter the properties of the API and the carrier. Therefore, solid state characterization is inevitable as a tool in gathering information, resulting in the production of a stable inhalation product [40].

Generally, particles can be crystalline or amorphous. Earlier developed DPI formulations mostly consisted of pure crystalline particles. Crystals are thermodynamically stable, non-spherical and have low surface energy, but they tend to pack more tightly due to high density. Recent research has shown that amorphous particles have properties that can ensure increased therapeutic effect. The disadvantages are their instability and high sensitivity to different environmental conditions, resulting in changes which might be of great concern in DPI systems [10, 41].

The analysis of the surface chemical properties and thermodynamics is of high importance. For instance, surface energy strongly influences the aerosol performance of powders. The higher the surface energy of the powder, the higher the adhesion or cohesion forces will be. This can lead to the formation of agglomerates with higher strength and a decreased level of de-agglomeration [27].

Besides crystallinity and surface energetics, one more indicator for the stability of amorphous solids is the glass transition temperature, Tg. This is a critical physical property, which can greatly alter the stability of the system together with viscoelastic properties. The glass transition is reversible in amorphous materials and crystallization is accelerated above this temperature [42]. Whether the transition from amorphous to crystalline will occur spontaneously or not, depends on the mobility of the molecules. When the molecules are below the Tg, they will lack enough mobility for spontaneous transition. However, this doesn't mean that transition will not take place; it will, but only after a longer period of time [18].

Water can decrease the Tg of the material because it acts as a plasticizer, which leads to spontaneous recrystallization of the formulation.

Many theories exist about the plasticization mechanism but the most common one is the free volume theory. This theory states that glass transition occurs when the powder has a certain free volume. When material absorbs water, Tg will become lower and the presence of small molecules will increase the free volume of this system, thereby increasing the flexibility of the material.

Concerning stability, this lowering can transform a stable product to a highly unstable one. Hence, long exposure to atmospheric water or inadequate storage at high humidity might be a source of change of in the DPI formulations [44].

In favor of improvement of existing formulations, it is of high interest to understand how the secondary processing of the API and the carrier influence all parameters mentioned before.

1.3.5. Aim of the study

Considering all parameters mentioned before, it can be concluded that a crucial factor in dry powder inhaler formulations is the particle size of active pharmaceutical ingredient (API), together with the API solid-state and forces involved in attaching and detaching the API to/from the carrier.

Therefore, the aim of this study was to understand the effect of secondary processing of the API on its solid-state and interparticulate forces acting between the carrier and the API and between the API particles itself. Salbutamol sulphate

was used as model API, while mannitol was employed as model carrier. The present work investigated the solid-state of jet milled and spray dried salbutamol sulphate and the influence of different material properties on the inhalation formulation, mainly the blending behavior and its aerodynamic performance. Additionally, the solid-state characterization was performed at different time points and under elevated humidity conditions. The intention was to investigate eventual occurring changes as a result of increased relative humidity and the change of formulation performance over time. Inhalation performance of the formulation was determined by use of the NGI, obtaining the aerodynamic particle size distribution (APSD) and the fine particle fraction (FPF). Furthermore, surface analysis of the formulations has been conducted. Shape and surface morphology of the mixtures were qualitatively examined via SEM in order to examine the influence of the different shape of the particles on the mixing performance and API distribution over the carrier particles.

2. Materials and Methods

2.1. Materials

Crystalline salbutamol sulphate was purchased from Selectchemie AG (Zurich, Switzerland) in USP25 quality and it was used as model API after jet milling and spray drying. As a model carrier, crystalline β-mannitol (Pearlitol 160C) was used as received from Roquette (Freres, Lestrem, France). Acetic acid, absolute ethanol, Tween 20 were purchased from Sigma-Aldrich (Munich, Germany), while capsules size 2 were supplied by Capsugel.

2.2. Secondary processing of the API

2.2.1. Jet-milling

Jet-milling of SS was performed in a 50 AS spiral jet mill (Hosokawa Alpine, Augsburg, Germany). Crystalline SS was milled using an injection pressure of 8.0bar and a milling pressure of 5.0bar. These conditions were suitable for generating the particles of 1-5μm in size.

2.2.2. Spray Drying

SS was spray dried with a Nano Spray Dryer B-90 (Buechi Labortechnik AG, Flawil, Switzerland) equipped with the long version of the drying chamber. Spraying conditions were chosen according to previous work of Littringer and Zellnitz [43]. Within these conditions, spherical particles of SS were prepared. In order to obtain particle size between 1-5μm, a spray head mesh of 5.5μm was used. Feed concentration was 7.5% and the flow rate was set to 110L/min with spray intensity of 30%. An aqueous solution of SS was prepared with purified water (TKA Wasseraufbereitunssysteme GmbH, Niederelbert, Germany).

2.3. Solid-state characterization of the API

As mentioned before, the solid-state of the API is an important aspect of the drug stability and its therapeutic performance. All analysis except the particle size analysis and the contact angles were done with two different storage conditions. Saturated salt solutions were prepared and put in the desiccator to create a humidity chambers. The nominal relative humidity (RH) values were 11% ($LiCl_3$) and 43% (K_2CO_3) and the samples were stored at 25°C. Hygrometer readings showed slightly higher values, they were approximately 18 and 45%, respectively. This might be due to the higher relative humidity of the storage room. The samples were tested from time 0 (the day when the secondary processing was performed) to 21st day.

2.3.1. Particle size analysis

Particle size analysis has been conducted to ensure that inhalable size particles (1-5µm) were obtained after secondary processing. The analysis was done via laser diffraction (Helos/KR, Sympatec GmbH, Clausthal-Zellerfeld, Germany). The powder was dispersed with dispersion pressure of 3.0 bar, with a dispersion unit (Rodos/L, Sympatec GmbH, Clausthal-Zellerfeld, Germany) and a vibrating chute (Vibri, Sympatec GmbH, Clausthal-Zellerfeld, Germany). The sampling time was 10 seconds with measurement range R2 (0.45-87.5µm). The data was evaluated with use of Windox 5 (Sympatec) software.

2.3.2. Small and wide angle X-ray scattering (SWAXS)

Small and wide angle X-ray scattering was used to determine crystallinity of the spray dried SS. WAXS measurements were performed using the Microcalix (Bruker AXS, Karlsruhe). Exposure duration was 600s and samples were analyzed at 25°C, 120°C, 170°C, 200°C and after 30min again at 200°C. The obtained results were compared with crystalline SS.

2.3.3. Contact angle measurements

In order to obtain the surface free energy of the powder, contact angles were measured. The contact angles of jet-milled and spray dried SS were measured using a Tensiometer K100 (Krüss GmbH, Hamburg, Germany) by Wilhelmy plate technique as previously described by Pinto et al. [30]. For this technique a rectangle shape substrate was used, coated with a double-side tape and the samples were uniformly coated onto its surface. The system of three liquids was used where two polar liquids were water and ethylene glycol, while the non-polar liquid was diiodomethane. For each liquid, three measurements were done. The liquid was placed in a glass dish and raised by the motorized platform to contact the powder plate which was hanging perpendicular to the surface of the liquid. The speed of the platform raising was 6mm/min. Evaluation of the data was performed with Krüss Laboratory Desktop software (Krüss GmbH, Hamburg, Germany). The surface free energy of the solid was calculated using the Good and van Oss equation.

2.3.4. Fourier Transform Infrared Spectroscopy (FTIR)

As a qualitative technique for determination of the sample crystallinity of the sample, FTIR was used. Spectroscopy analysis was done with FTIR Vertex 70 (Bruker Austria GmbH, Austria). Spectra were recorded by OPUS software. FTIR scattering between 600-3800cm^{-1} was recorded with 16 background scans and 64 scans of the sample. Each sample was measured 3 times and averaged. An atmospheric correction in the software was done in order to compensate CO2 and H_2O.

2.3.5. Differential Scanning Calorimetry (DSC)

Modulated temperature DSC (DSC 204 F1 Phoenix, Netzsch, Selb, Germany) experiments were done to determine the glass transition temperature of the samples. The samples were heated from 25°C to 230°C with a heating rate of 5°C/min in hermetically sealed pans. Approximately 3-5mg of the sample was measured with the high precision scale (XP205DR, Mettler Toledo GmbH Vienna,

Austria). The evaluation of the obtained thermograms was done with NETZSCH Proteus Thermal analysis software, version 6. 1. 0.

2.3.6. Optical Microscopy

Optical microscopy has been done to obtain data about the surface morphology of the particles. The aim was to investigate any change that might exist between different time points and relative humidity of the sample and how that might impact the crystallinity of the sample. The sample was dispersed on a glass slide and the magnification was set to 20x. Furthermore, hot stage microscopy has been done to study the change of the spray dried SS sample as a function of temperature and time. Heating of the sample started at 25°C to 230°C with a heating rate of 5°C/min. Sampling time was 30s up to final 2460s. Both analyses were done using Hot Stage Raman Microscope (Senterra, Bruker Austria GmbH, Vienna, Austria).

2.4. Preparation and characterization of the mixtures

2.4.1. Preparation of adhesive mixtures

Adhesive mixtures of 2% spray dried and jet-milled SS were prepared. 9.80g of Pearlitol 160C and 0.20g of the API were weighed into the metal vessels using the sandwich method. The first 5.0g of the carrier was weighed in the vessel followed by a layer of the API and then the rest of the carrier. The vessels were blended with Turbula blender TC2 (Willy A. Bachofen Maschinenfabrik, Muttenz, Switzerland) for 60 min at 62 rpm. Mixtures were prepared at time 0, after 7 and 21 days after secondary processing and stored for 24h in the desiccator with saturated salt ($LiCL_3$) solution before further analysis. For each time point, 3 mixtures were prepared.

2.4.2. Mixing homogeneity

Homogeneity of each mixture was determined by taking 10 samples of approximately 45mg and dissolved in 20ml of the acetic acid buffer (pH=3). Samples were taken from the top, center and bottom of the vessel, ensuring the

uniform sampling. For the analysis of the dissolved samples, high performance liquid chromatography (HPLC) was used.

2.4.3. Scanning electron microscopy (SEM)

The morphology of adhesive mixtures was examined using a scanning electron microscope (SEM) (Zeiss Ultra 55, Zeiss, Oberkochen, Germany) operating at 5kV. Prior to analysis, samples were gold palladium sputtered.

2.4.4. Evaluation of aerodynamic performance

The aerodynamic assessment of fine particles was evaluated using the NGI (Copley Scientific, Nottingham, United Kingdom). The analysis was performed according to the European Pharmacopoeia (preparations for inhalation: aerodynamic assessment of fine particles, Ph. Eur., 7.0). Based on the previous work of Faulhammer et al. [39] similar conditions were established. For analysis purpose, the small trays and the large cups were coated with the coating agent (2% solution of Tween 20 in absolute ethanol) using 2ml and 4ml of the coating agent, respectively. The pre-separator was filled with 10ml of acetic acid buffer (pH=3). As an inhalation device, Aerolizer® was used. The pressure drop of 4.0kPa could not be achieved because of low resistance inhaler use. Therefore, a flow rate of 100ml/min was adjusted. In order to control the pressure of closed NGI, a leak test was performed before each experiment. Within 60s, pressure must not increase more than 2.0kPa. During the experiments, the solenoid valve of the critical flow controller (TPK, Copley Scientific, Nottingham, United Kingdom) was kept open for 2.4s ensuring that 4l of air was sucked with the help of a pump (SV1040, Busch, Chevenez, Switzerland) through the apparatus. Capsules used for analysis were previously conditioned for 24h in a desiccator over a silica gel. Prior to the experiment, they were filled with the adhesive mixtures. For each mixture, 4 capsules of size 2.0 were filled manually with approximately 45mg of the sample. Then a capsule was placed into the compartment of the inhaler in which powder was released by piercing the capsule by pushing two buttons on the inhaler base, followed by powder discharging into the impactor. The inhalation device, induction port and mouthpiece were rinsed with 10ml of the buffer. Moreover, the pre-separator was rinsed with 50ml of the

buffer. The active on the cups was dissolved in 10ml of the buffer. Each mixture was tested in triplicate. The amount of drug in the mouthpiece plus the introduction port, the pre-separator, the inhaler and in each tray were determined via HPLC. The fine particle dose (FPD), the emitted dose (ED) and the fine particle fraction (FPF) were calculated according to European Pharmacopoeia. FPD gives the amount the API with an aerodynamic diameter smaller than 5µm, ED is the drug found across the whole impactor and FPF is the ratio of FPD to ED.

2.4.5. HPLC analysis

The samples were analyzed by HPLC on a Waters 2695 (Milford, USA) HPLC system equipped with a Waters 2996 photodiode array detector and an autosampler. The mobile phase consisted of 60% A: 5mM hexanesulfonic acid sodium salt in water + 1% acetic acid and 40% B: methanol. UV-detection has been done at 267nm. As stationary phase a Phenomenex Luna C18 5µm 100A column was used. The column temperature was 30°C and a sample solution aliquot of 50µl was injected into the system. These conditions were proven optimal for this analysis according to Zellnitz et al. [45]. Each sample was analyzed two times. A calibration curve, consisting of six solutions of known concentration was recorded.

3. Results and Discussion

3.1. Influence of secondary processing on the solid state of the API

3.1.1. Particle characterization

In order to understand the effect of secondary processing on micrometrics, physical properties of the spray dried and jet-milled SS were investigated such as particle size distribution and particle morphology. For comparison, crystalline SS starting material was used. Table 1 shows the particle size distribution of the API.

Table 1: Particle size distribution of API powders

	X_{10} (µm)	X_{50} (µm)	X_{90} (µm)	Span
Spray Dried SS	0.64	3.88	8.76	2.09
Milled SS	0.40	1.23	3.23	2.30
Crystalline SS	1.13	7.20	20.65	2.71

As both spray dried and jet-milled SS particles exhibit x_{50} below 5µm, it can be concluded that they are suitable for deep lung penetration after inhalation. Generally, when comparing jet-milled and spray dried sample, the PSD is slightly higher for spray dried sample than for the jet-milled samples. This indicates that different profiles of lung penetration might be possible.

The span value was calculated by means of the difference in particle diameters X_{90} and X_{10} divided by X_{50}. The smallest value of 2.09 was obtained for spray dried SS. These findings show that spray drying is a more controllable process than jet-milling and that by carefully selecting the processing conditions, spray drying can produce particles with narrow size distributions.

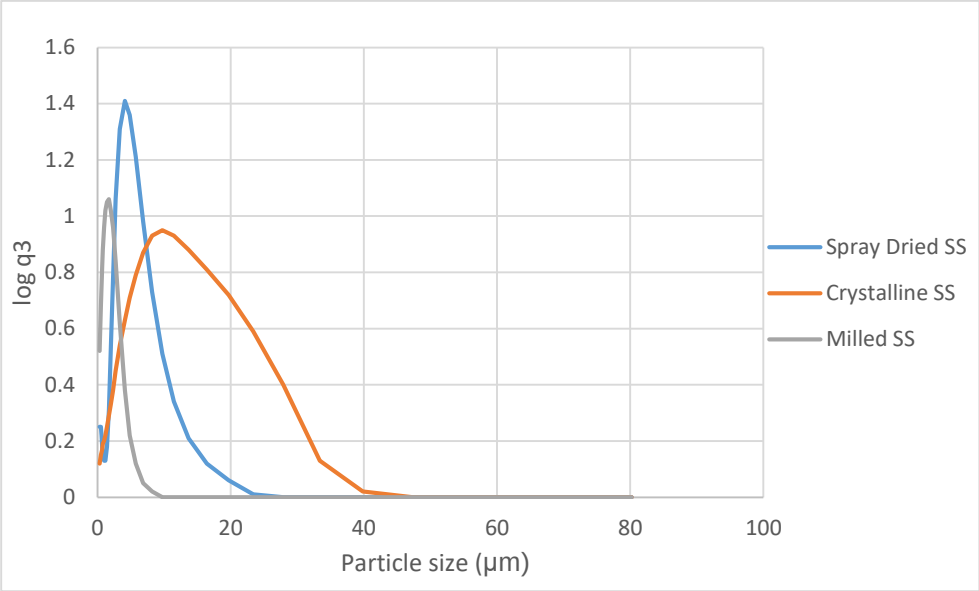

Figure 9: Frequency volume based particle size distribution

Figure 9 illustrates the narrower particle size distribution of the spray dried as well as the jet-milled SS sample. Overall, when compared with SS starting material, a significant decrease in the particle size can be observed for both spray-dried and jet-milled API.

Particle shape was determined by optical microscopy.

Figure 10 shows the crystalline SS starting material and its needle shape habit. Figure 11 and 12 show images obtained at different time points. It can be seen that SS, maintain the needle-like shape (Figure 11 b)) after jet-milling whereas spray dried SS has a spherical shape (Figure 12 b)).

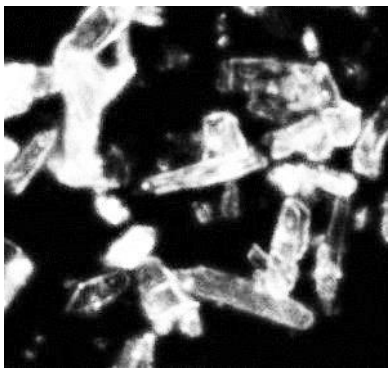

Figure 10: Crystalline SS

As mentioned before, one purpose was to investigate possible changes due to different storage conditions and the stability of the API after a certain time period.

Stability study at 18% RH:

When comparing the different time points between samples, it was observed that particles in both spray dried and jet-milled sample near each other and become more compacted with time. As a result, it seems that certain particles are fused together. Furthermore, during microscopic analysis, it was observed on the macroscopic level that samples were sticky and more compacted than at time 0. Overall, the jet-milled material appeared to maintain the same morphology as at time 0. However, spray dried particles display slightly different morphology over time, what can be observed when comparing time 0 with results after 21 days (Figure 12 a) and e), marked with red circles). This might indicate sample instability and a tendency towards agglomeration. Considering that spray dried SS powder was not additionally dried after the process, it is possible that certain amount of water remained in the sample. In the literature, the formation of sinter bridges was studied as a mechanism for the formation of agglomerates. At lower temperature, sintering is a result of surface diffusion. After initial contact, adherence of particles occurs due to the weak forces such as Van der Waals or agglomeration forces which originate from liquids [46, 47]. Further analyses were performed in order to confirm this hypothesis.

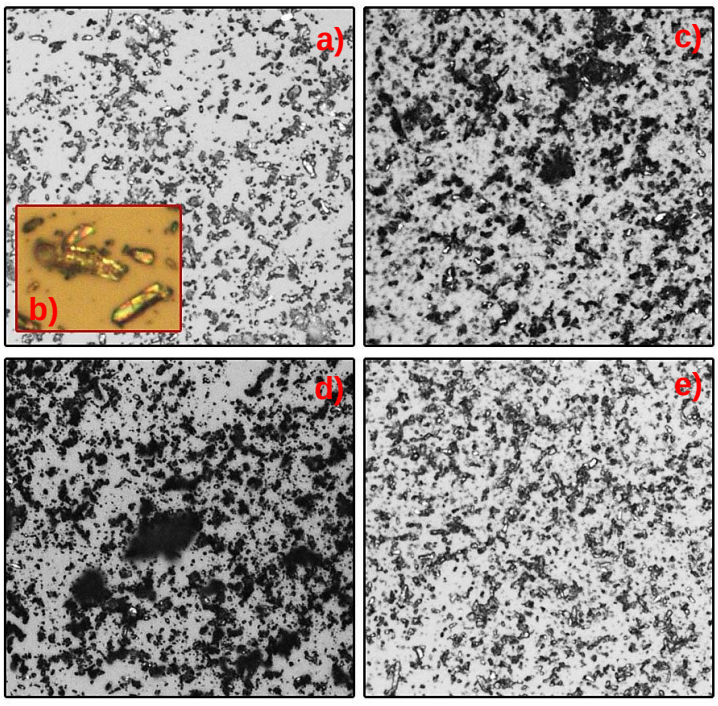

Figure 11: Milled SS: a) time 0, b) characteristic needle-like shape, at close range for better clarity, c) after 7 days, d) after 14 days, e) after 21 days

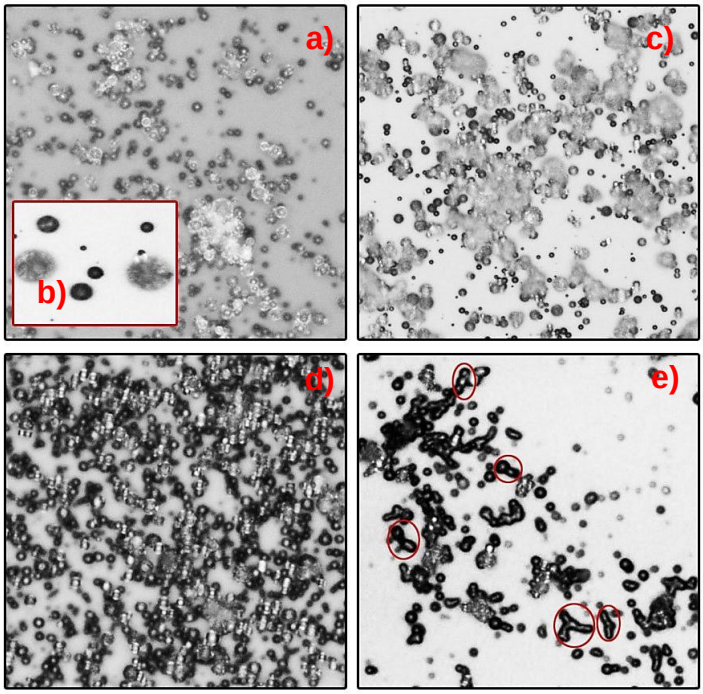

Figure 12: Spray Dried SS: a) time 0, b) characteristic spherical shape, at close range for better clarity, c) after 7 days, d) after 14 days, e) after 21 days

Stability study at 45% RH:

As mentioned before, due to high relative humidity particles can form viscous bridges between them (phenomena known as sintering), possibly leading to the formation of agglomerates. Figure 13 illustrates how the jet-milled sample behaves under high relative humidity conditions. It can be concluded that morphology of the particles remains the same. However, the presence of sinter bridges can be noted, especially comparing time 0 with day 21. Similar findings are shown in Figure 14 for the spray dried samples. It can be assumed that due to amorphous nature of spray dried SS, the sample might have absorbed more water when compared with crystalline, jet-milled SS sample. As a result, the faster formation of sintering bridges occurred. In Figure 14 b), slight changes in morphology of the particles are visible. Comparing with data obtained when analysis was done at low relative humidity, this effect is visible significantly earlier at 48% RH (day 21 and day 14, respectively). Nevertheless, this phenomenon was only obtained partially and not throughout the whole bulk powder.

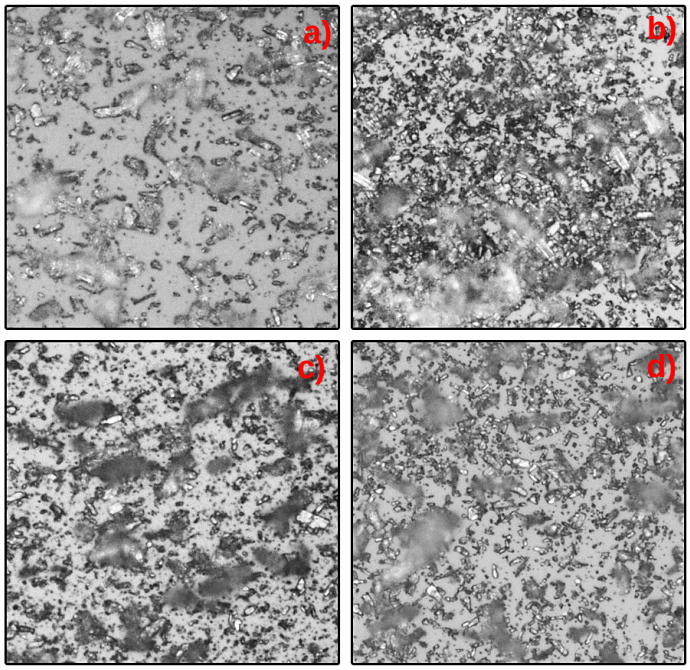

Figure 13: Milled SS a) time 0, b) after 7 days, c) after 14 days, d) after 21 days

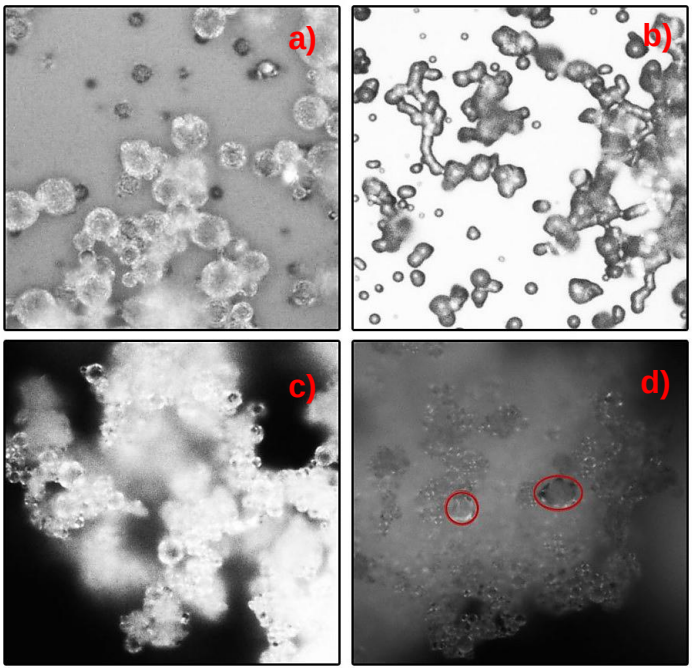

Figure 14: Spray dried SS a) time 0, b) after 7 days, c) after 14 days, d) after 21 days

From optical inspection of the samples, it can be hypothesized that water was absorbed by the samples, expressed more in spray dried than milled SS sample. Taking into consideration that water might act as a plasticizer, decreasing the glass transition temperature and leading to sample recrystallization, the observed changed morphology could be the sign of former.

3.1.2. Investigation of the API solid-state

FTIR, SWAXS and MTDSC were employed as methods to determine the solid state of salbutamol sulphate particles after secondary processing.

The effect of secondary processing on the crystallinity of SS is widely researched [41-44]. Results from the present work are in accordance with previous finding in literature. After jet-milling SS particles show a crystalline structure whereas after spray drying SS becomes amorphous. These findings are supported by SWAXS as well as with FTIR results.

SWAXS analysis

In order to better understand the solid-state of the spray dried sample, WAXS measurements were performed. Considering that amorphous powders lack long-range order in their structure, their pattern is unlike a crystalline powder and amorphous halo can be noted [47]. Figure 15 shows WAXS patterns of crystalline starting material and spray dried samples. The spectra contain the characteristic Bragg peaks of the crystalline form (starting material), for instance, at 20.63°, 21.98° and 23.74°. For the spectrum of the spray dried sample, amorphous halo is visible. Furthermore, WAXS analysis showed that the spray dried sample remained amorphous throughout the analysis time of 21 days (data not shown). No Bragg peaks could be noted, indicating the same solid-state form of the sample. However, comparing with patterns of the crystalline sample, a significant difference has been observed. As mentioned before, the crystalline sample shows clear peaks, whereas, the spectrum obtained for spray dried sample does not show these peaks, confirming that samples obtained via spray drying are amorphous [39].

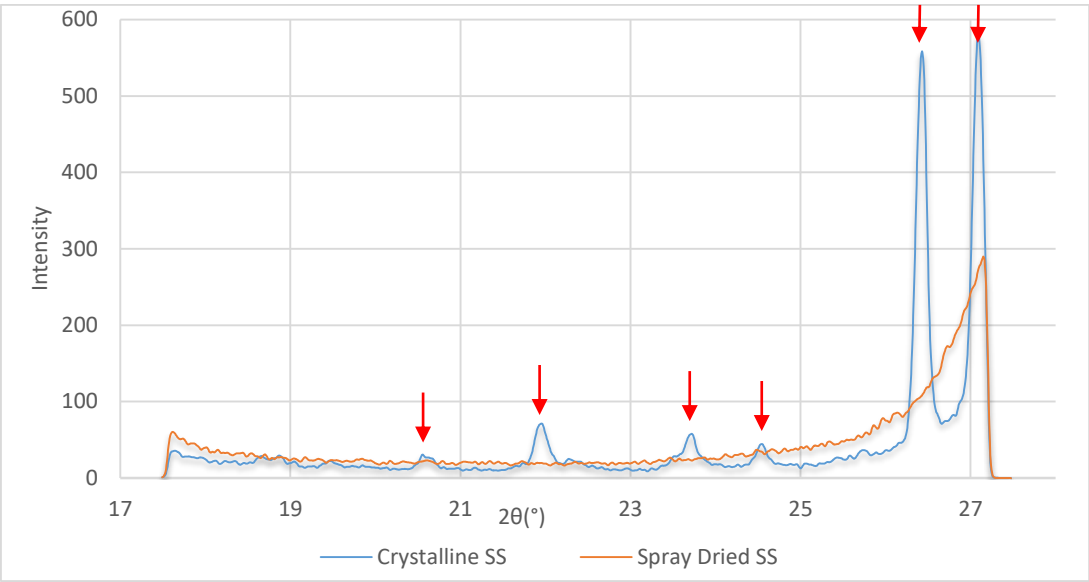

Figure 15: WAXS patterns of crystalline and spray dried SS, T=25°C

FTIR analysis

Further analysis of the jet-milled and spray dried SS was carried out using FTIR to confirm the solid-state of the particles. Figures 16, 17, 18 and 19 show the resulting spectra.

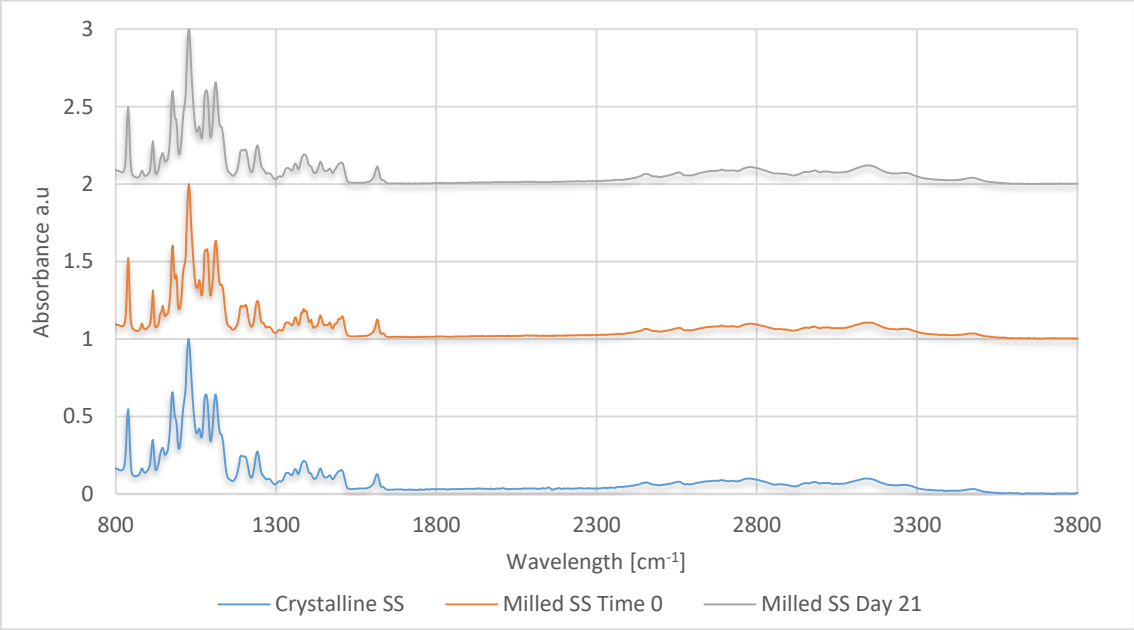

Figure 16: FTIR spectra for milled SS stored at 18% RH

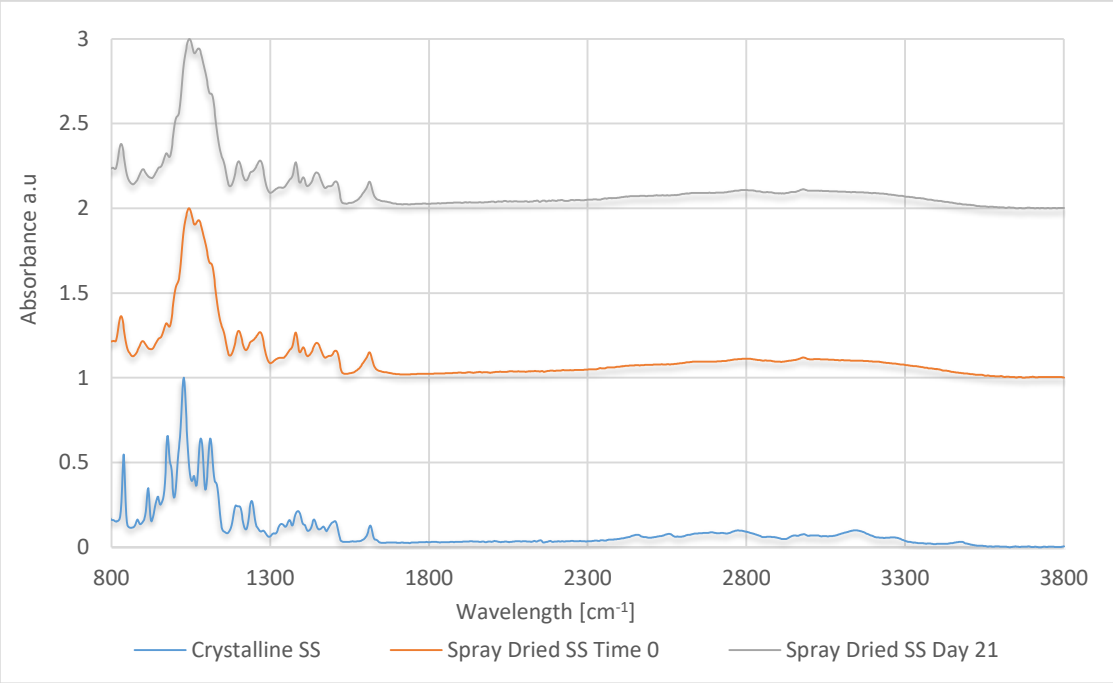

Figure 17: FTIR spectra for spray dried SS stored at 18% RH

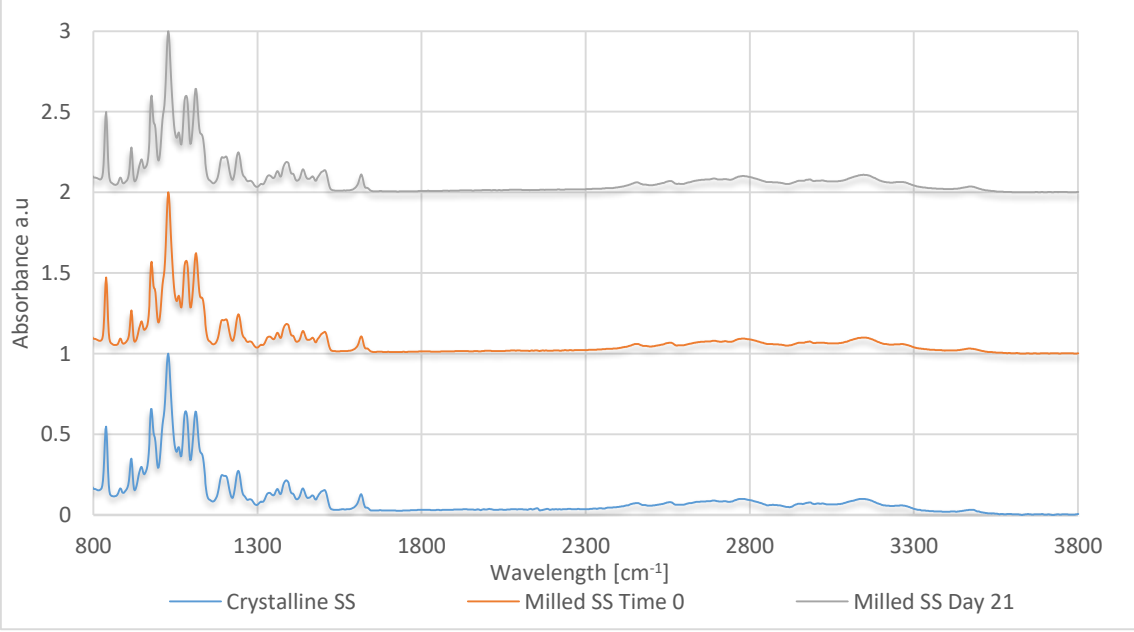

Figure 18: FTIR spectra for milled SS, stored at 45% RH

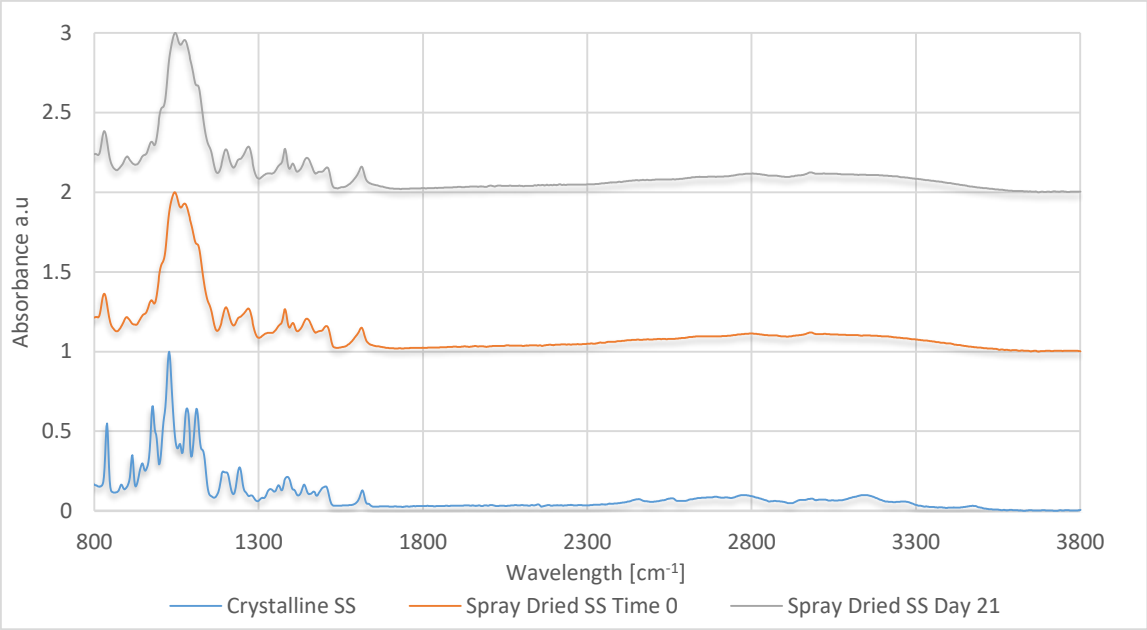

Figure 19: FTIR spectra for spray dried SS, stored at 45% RH

The FTIR spectra can be interpreted according to different wavenumber regions. In Figure 16, 17, 18 and 19 the comparisons of jet-milled and spray dried material with the crystalline starting material are shown. Milled SS sample shows peaks which are characteristic for crystalline materials. The 1100-1800cm^{-1} region is a very important spectroscopic region because it shows the vibration from C=C stretch in the ring (it occurs at 1616cm^{-1}) followed by bands at 1558cm^{-1} and 1205cm^{-1} which are the result of C-OH coupled with the phenyl ring vibrations. In the 3800-2200cm^{-1} region, the OH (at 3474cm^{-1}) and NH (3280-3160cm^{-1}) (Figure 20, marked with red circles) stretching band can be observed. However, spray dried samples exhibit broad and wide peaks when compared to the sharp peaks observed for the crystalline material, illustrating a lack of long-range molecular ordering, thus confirming the amorphous state of these samples [48,49].

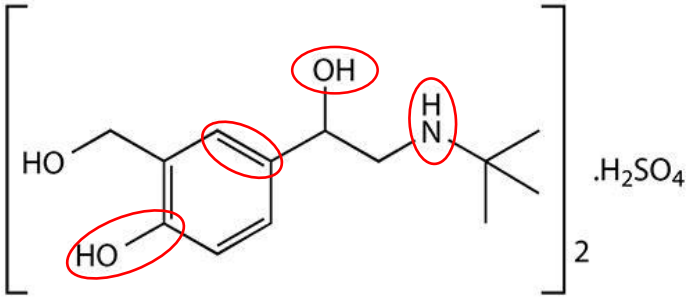

Figure 20: Structural formula of SS

Furthermore, both jet-milled and spray dried samples were stable during the analyzed period. The resulting spectra after storing at 45% relative humidity are comparable to the ones at low relative humidity over time. Grisedale et al. reported recrystallization event as a result of storage conditions of 54% relative humidity where new absorption peaks were clearly seen in the area between 3500-2500cm^{-}1 [44]. In Figure 19 no new absorption peaks were observed in this region, thus implying that recrystallization did not occur under this level of humidity. Moreover, Zellnitz et al. described recrystallization of amorphous salbutamol sulphate particles after exposure at 60% relative humidity, confirming that a level of 45% is too low to cause recrystallization [50].

MTDSC was used as a method employed in the examination of effects of secondary processing on the behavior and structure of SS under different temperature conditions. Investigation on the glass transition was done, in terms of variability of the Tg values and eventual recrystallization. All measurements were done in duplicates.

MTDSC analysis

Table 2 and 3 summarize the data for the milled and spray dried sample, respectively, including the onset temperature values obtained from the heat flow signals.

Table 2: MTDSC results for milled SS

	Time 0	Day 7	Day 14	Day 21
Onset Temperature Tg 1 ± s.d. (°C)	60.65±2.05	58.55±1.34	48.7±7.78	60.85±9.40

It can be noted that values for the glass transition temperature changed slightly over time, indicating that a very small amorphous fraction was generated during jet-milling, and remain as so (no recrystallization) throughout the analysis time. During analysis of the obtained thermograms, the detection of the onset temperature was difficult. Considering the detection limit of the DSC method, it is often hard to detect very low levels of amorphous materials (below 10% w/w) [47].

The low detection limit is a result of the fact that DSC as a method measures the entire sample. Therefore, small amorphous fractions become a small part of the total signal which is tough to distinguish from the noise signals [18].

Table 3: MTDSC results for spray dried SS

	Time 0	Day 7	Day 14	Day 21
Onset temperature Tg 1 ± s.d. (°C)	50.15±0.50	51.10±0.14	53.45±0.07	54.25±1.91
Onset temperature Tg 2 ± s.d. (°C)	68.90±0.70	62.00±0.14	63.75±0.07	63.30±1.27

The data obtained for spray dried samples show a slight increase of the first glass transition temperature. Moreover, two glass transitions are visible in the MTDSC reversing heat flow. This is only visible when sealed pans are used for analysis. One possible explanation for this phenomenon is the existence of two distinct structural relaxation regions, containing different water quantities. These regions can be related to hydrated bulk and dry surface. Water molecules migrate between the molecules of the amorphous powder having a plasticizing effect. Therefore, the first glass transition might be a consequence of plasticized regions within the bulk whereas the second one of the less plasticized region created on the surface. When using the pinholed pans, water can easily escape the sample thus negating this effect [44].

A second explanation could be the formation of sinter bridges between particle's surfaces. When particles are in contact, due to the difference in capillary pressure at the contact point they could diffuse towards each other, forming so called sinter bridges [51,52]. It could be assumed that these bridges have less quantity of water compared to the particle bulk thus leading to the second glass transition event.

In order to confirm this hypothesis, analysis of spray dried samples was performed under elevated humidity conditions (Table 4).

Table 4: MTDSC results for spray dried SS, stored at RH=45%

	Time 0	24h	Day 7	Day 14	Day 21
Onset temperature Tg 1 ± s.d. (°C)	47.15±0.92	31.4±0.42	39.80±2.67	30.50±0.99	35.75±1.48
Onset temperature Tg 2 ± s.d. (°C)	67.85±0.07	48.55±2.74	51.90±0.99	52.25±1.34	49.95±1.77

Interestingly, the first glass transition event is visible at lower temperatures when compared with the same analysis at lower humidity. The reason, therefore, might be a higher level of water content in the sample due to higher storage humidity, leading to Tg lowering. It is necessary to highlight that actual water content in the samples was not determined, thus this hypothesis can't be supported by results. Moreover, the appearance of a second glass transition is visible already after the spray dried process (Time 0) implying the rapid formation of sinter bridges. A possible explanation might be a higher level of water content in the sample, not only from surrounding humidity yet from the spray drying process itself. For instance, humidity of air used in the drying process, as well as the time of drying, were not controlled and held constant for each spray drying experiment. A higher water content would lead to a higher molecular mobility and facilitate molecular surface diffusion between particles, causing sinter bridging. Furthermore, the values of the glass transition when samples are stored at 45% relative humidity were noticeably lower when compared with values for samples stored at 18% relative humidity, indicating higher levels of absorbed water in the samples.

Grisedale et al. reported a decrease of the second glass transition event after storage, indicating that particles reached the equilibrium with surrounding humidity, forming a homogenized powder resulting in a single Tg [44]. In this

study, this could not be observed. A possible reason might be the difference in the level of storage humidity, 54% to 45% respectively.

Additionally, it can be observed that the Tg values were considerably lower after 24 hours of storage when comparing time 0 and 7 days results. This could yet again be explained with levels of water in the sample. After 24 hours, the sample might have absorbed a substantial amount of water on the surface, which is then sampled for the analysis, resulting in lower Tg values. After 7 days storage, water could have migrated throughout the sample, thus when sampling, the sample contained less quantity of water, resulting in increased Tg value. Even though the water content measurements were not part of this study, this hypothesis can be based on many previous studies. For example, Kaialy stated that amorphous particles have higher moisture content because their structure is less dense and have higher free volume in which water can pierce easily [53].

Figure 21 shows the appearance of a spray dried sample and its change with time and temperature. Compared to the beginning of the analysis (Figure 21a)), different degradation phases of salbutamol sulphate are visible with increasing temperature (Figure 21 c, d, and e). Sonvico et al. described the degradation mechanism of SS shown in Figure 22 [54].

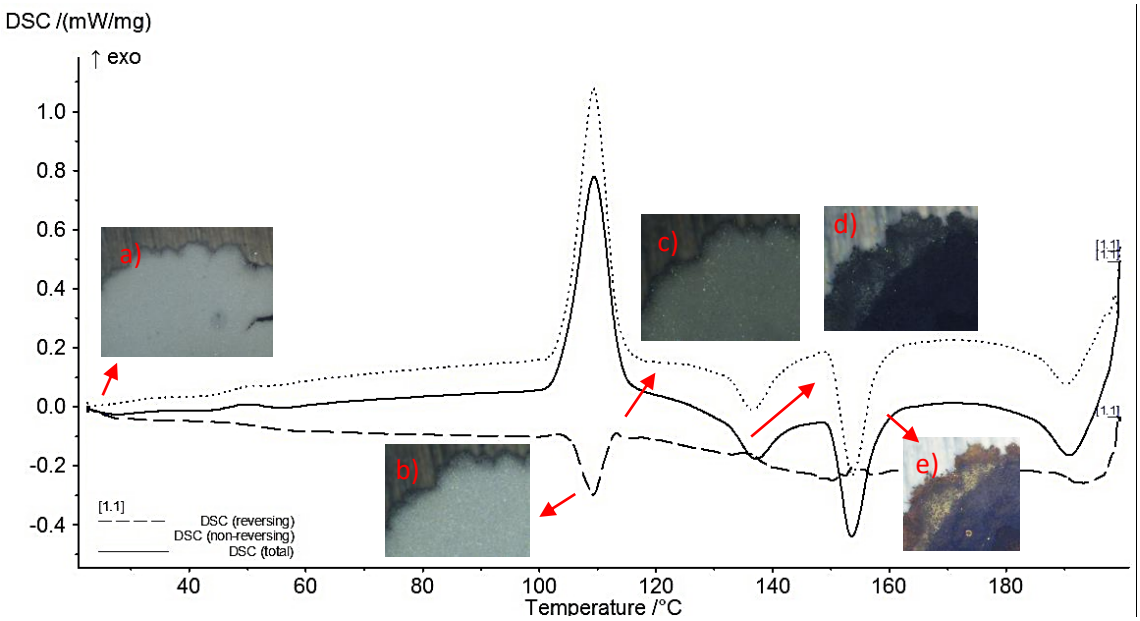

Figure 21: Hot Stage Microscopy with thermogram of spray dried SS comparison a) beginning of analysis, b) recrystallization peak, c), d) and e) degradation phases of SS

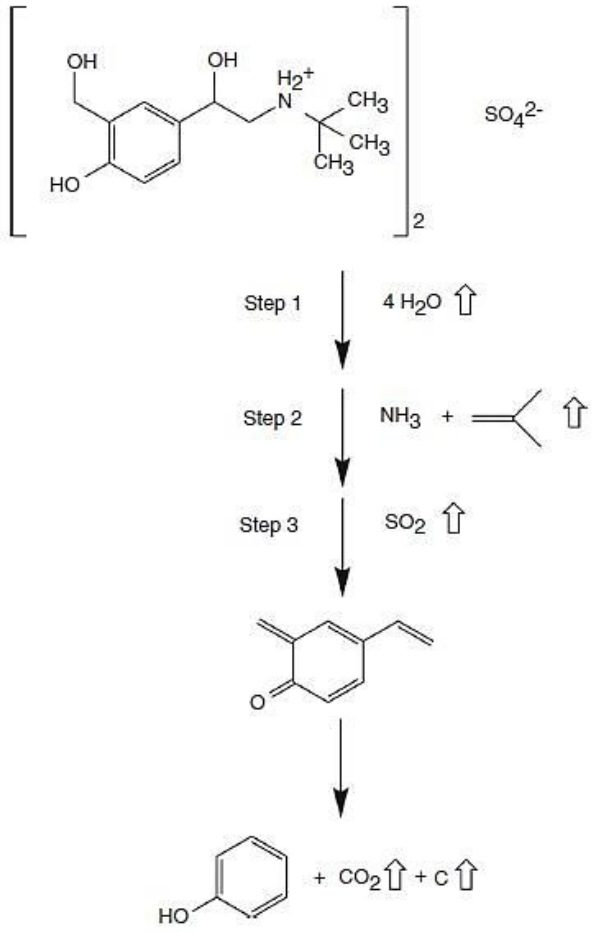

Figure 22: Degradation mechanism of SS during heating; adapted from [54]

The degradation mechanism of SS can be explained by three main steps, occurring at different temperatures. In the first step, SS molecules dehydrate by losing the two molecules of water, evident around 200°C. A second step can be attributed to ammonia, appearing around 260°C, followed by the formation of sulphur dioxide. The main degradation phases are characterized by the formation of carbon dioxide and carbon, starting approximately at 270°C with degradation of the aromatic fragments [54]. In Figure 21, degradation steps can be observed at lower temperatures. This could be due to the fact that spray dried SS was used for the analysis, whereas in the study published by Sonvico et al. crystalline SS was analysed.

3.1.3. Surface energetics

Solid´s surface free energy was calculated using the Good and van Oss method using diiodomethane, water and ethylene glycol. Surface energetics (γ^{LW} γ^{+} γ^{-}) were calculated using the equation described in chapter 1.2.3. The system of

linear equations was solved using MatLab program (MathWorks, version 2015) with surface tension parameters taken from literature [55].

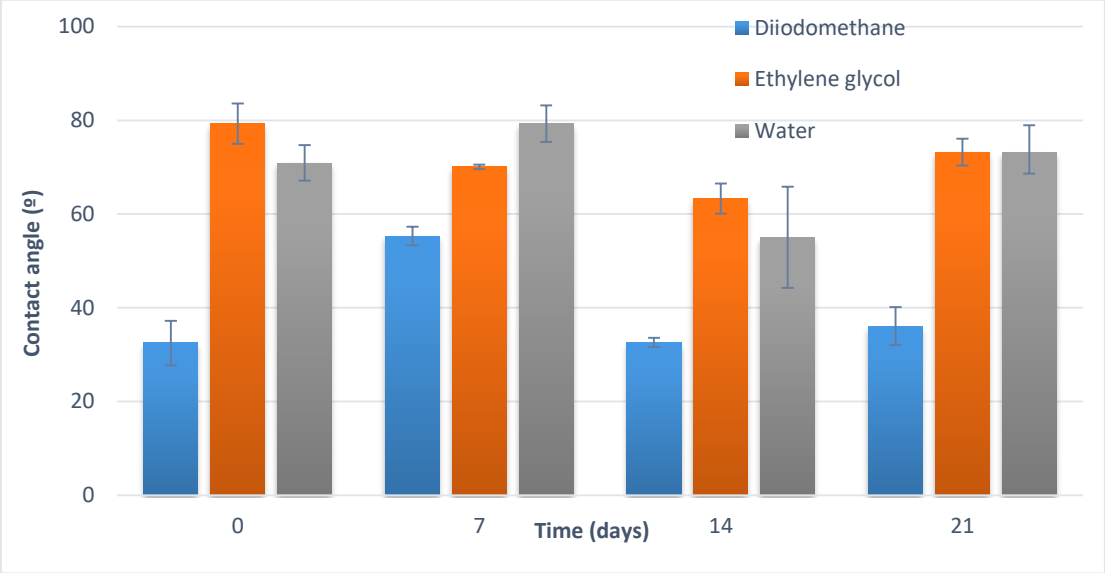

Figure 23: Graphical presentation of contact angles values for milled SS

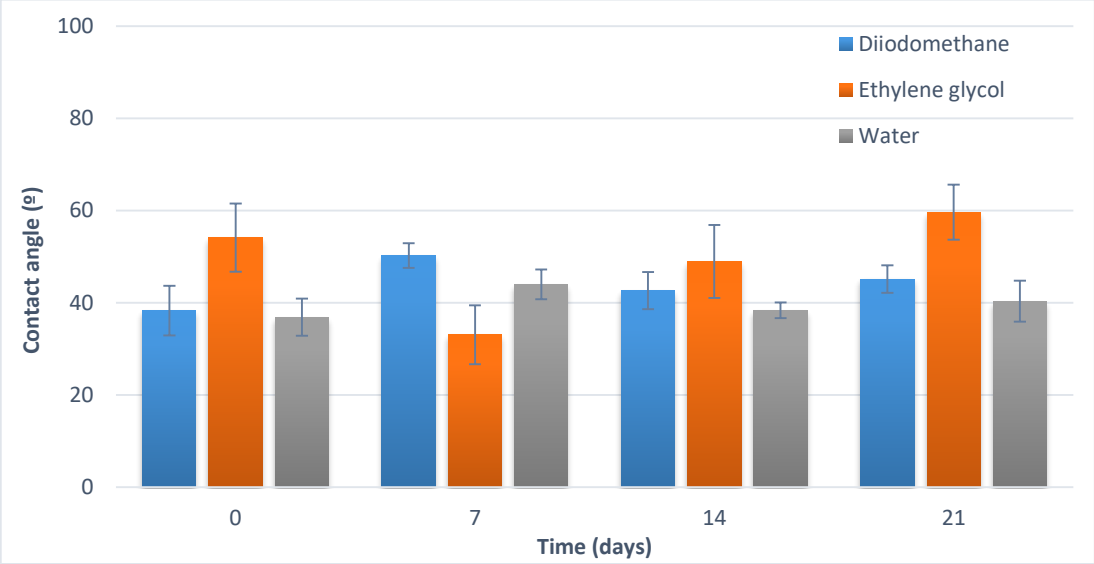

Figure 24: Graphical presentation of contact angles values for spray dried SS

Results in Figure 23 and 24 show lower contact angle value for spray dried samples comparing with jet-milled ones when polar liquids are used. Generally, lower contact angle values, when using polar liquids, can be attributed to the hydrophilic nature of SS [56]. More specifically, lower values of contact angles for spray dried sample might be explained with the solubility factor. As discussed

before, spray dried particles have an amorphous solid state, thus particles have high solubility. Higher solubility will lead to higher wettability of the particles, resulting in lower contact angle values [57,58].

Further, jet-milled SS show lowest values for non-polar liquid, suggesting that the API particles compose of more non-polar surface structures, with exposure of the hydrophobic trimethyl groups (Figure 25). Those groups will hold back the contracting motion of the liquid front when the liquid recedes, thus leading to a decrease in the observed contact angle [56].

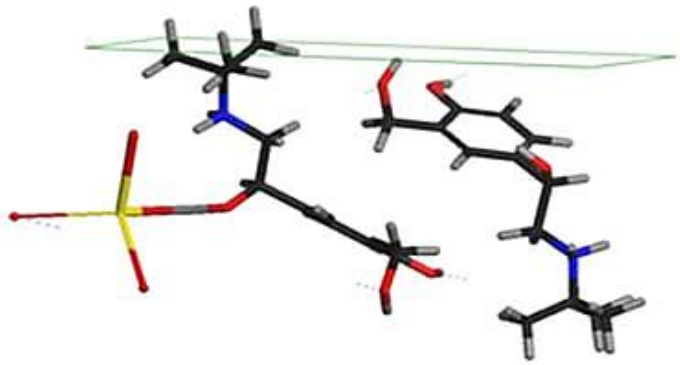

Figure 25: Molecular orientation of salbutamol sulphate; adapted from [59]

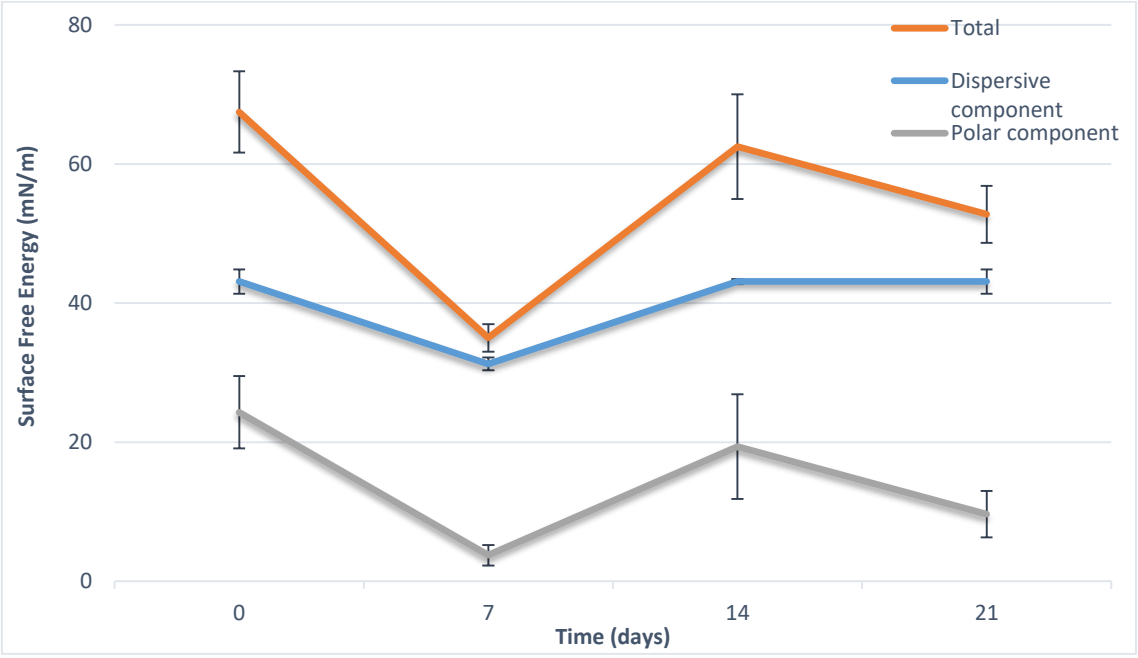

Figure 26: Graphical presentation of surface energy components, milled SS

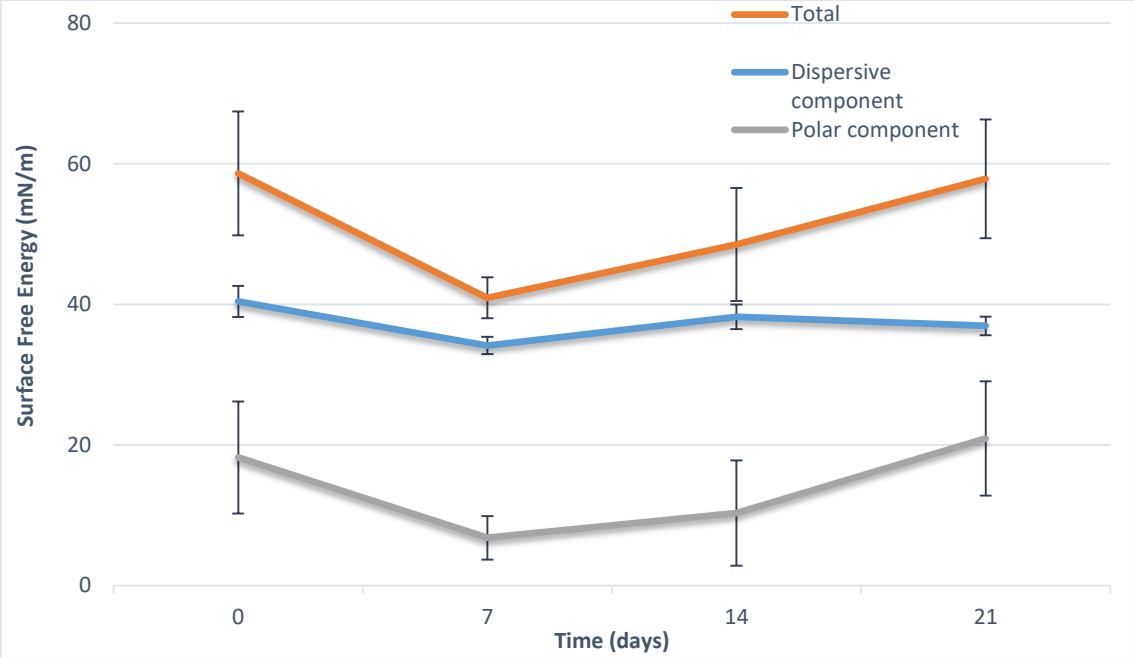

Figure 27: Graphical presentation of surface energy components, spray dried SS

Generally, spray dried SS particles showed similar surface energy values as jet-milled SS particles. A slight tendency of higher values for the jet-milled material could be observed (Figure 26 and 27). This is in accordance with literature. It is well reported that particles produced by milling have high surface energy [e.g. 27, 37]. The reason why this phenomenon could not be observed so clearly in the present study, might be sample agglomeration before the measurement. The powder was possibly not dispersed properly and consequently the measured values were results from formed agglomerates and not from single particles. Formation of agglomerates was observed on SEM images (discussed in chapter 3.2.2.). Moreover, during microscopic analysis, it was noted that samples were more compacted with time. Further, it can be observed, that surface energy values changed with time. Generally, data show a decrease in surface energy values after 7 days, followed by a slight increase of the values after 14 and 21 days. This was particularly evident for the milled sample.

These changes in surface energy over time can be explained when looking at the whole powder bed and powder bed packing. Until now, hypotheses were made by observing the individual particles and their behavior. When considering the

whole powder bed, more factors need to be taken into the account. Therefore, the interparticulate forces are considered throughout the whole powder bed, not only between individual particles, as well as the spatial orientation of the particles. Powder bed functionality will be reliant on the particle packing and micro-homogeneity of the interparticulate forces and small, cohesive particles will not be individually spread; they will exist as a continuous network structure [60]. Thus, decrease followed by the increase of the surface energy might be the result of powder bed packing. During sampling and the analysis, powder bed could be restructured into specific particle fractions which can be an assembly of agglomerated particles, resulting in lower surface energy than expected or into the primary particles which will exhibit higher surface energy.

3.2. Evaluation of adhesive mixtures and mixing homogeneity

Adhesive mixtures of 2% of the API were prepared and analyzed at different time points (at time 0, after 7 and 21 days). These time points were chosen according to results obtained via DSC and surface energy values.

3.2.1. Mixing homogeneity

For the mixing homogeneity and evaluation of the drug content, 10 samples were taken and analyzed via HPLC. The mixing homogeneity is expressed as the RSD in drug content. Results are presented in Table 5 and 6.

It would be expected that the weight percent of SS is 2% in the mixtures. However, analysis of the drug content in then mixture showed that weight percent varies at different time points as well as in mixtures within the same time point. Moreover, the drug content within the mixtures is inhomogeneously distributed, indicated by high relative standard deviation (RSD) for both spray dried and milled sample.

Table 5: Mean drug content and mixing homogeneity of adhesive mixtures with spray dried SS represented by RSD of mean drug content

Time point	Mean drug content ±RSD / %	Time point	Mean drug content ±RSD / %	Time point	Mean drug content ±RSD / %
Time 0	3.76±17.0	7th day	1.74±3.0	21st day	1.22±17.0
Time 0	4.29±4.0	7th day	1.70±3.0	21st day	1.91±4.0
Time 0	4.24±3.0	7th day	1.91±6.0	21st day	1.96±4.0

Adhesive mixtures containing spray dried SS show higher weight percent of SS at time 0, which might be explained as follows. Firstly, API particles are attached as large API agglomerates to the carrier, causing a higher value than expected. This hypothesis was supported with SEM images which are shown in chapter 3.2.2. Throughout the samples single spherical particles of SS were observed, however, in certain parts, agglomerates of the API were attached to the carrier. This could explain the relatively high RSD in the first mixture. It is possible that regions with a high number of agglomerates were sampled and consequently inadequate sampling caused errors and these high drug contents. Further, the effect of blending conditions was considered as a possible source. Kaialy reported that blending time, as well as speed, have a high impact on the mixing homogeneity. In general, increasing the time and speed of mixing could lead to improved homogeneity. However, API carrier interaction will reach equilibrium after a certain time, where further increase can lead to so-called de-mixing i.e. API will be detached from the carrier [21]. This finding can be applied here. It is possible that the mixing time was too long at time 0 and that API particles were detached from the carrier, leading to a sampling of the SS mostly without the carrier. This hypothesis is further supported by the result obtained after 7th and 21st day. The weight percent was close to 2% which can be explained by the formation of sinter bridges and agglomerates. The mixing speed and time were strong enough to break most of those agglomerates thus improving the homogeneity of the mixtures.

Table 6 shows the results obtained for mixtures containing jet-milled SS. It can be observed that weight percent of the API increases with time i.e. more API is attached to the carrier with time. Moreover, better attachment of the API with time could be visualized via SEM images. One possible reason is the same as already hypothesized for the spray dried samples. The chosen mixing conditions were suitable for breaking agglomerates that formed over time and were not present at time 0. At time 0 same mixing conditions might have been inappropriate or too strong to generate a homogeneous distribution of API particles. Relatively high standard deviation at time 0 could again be the result of bad sampling or inappropriate mixing conditions. Considering that for each mixture 10 samples were taken, the mass of the SS itself varied in those samples but overall weight percent was as expected.

Table 6: Mean drug content and mixing homogeneity of adhesive mixtures with milled SS represented by RSD of mean drug content

Time point	Mean drug content ±RSD / %	Time point	Mean drug content ±RSD / %	Time point	Mean drug content ±RSD / %
Time 0	1.76±52.0	7th day	2.12±13.0	21st day	2.15±13.0
Time 0	1.71±14.0	7th day	1.94±4.0	21st day	2.56±6.0
Time 0	1.51±29.0	7th day	1.13±8.0	21st day	2.01±5.0

Overall, obtained results showed high variations implying that mixing conditions must be optimized in order to achieve satisfactory mixing homogeneity and homogeneous drug distribution within the mixtures.

3.2.2. SEM images of adhesive mixtures

SEM analysis of prepared mixtures was performed for several reasons: to obtain additional information on the resulting particle morphology after secondary processing, to visualize the distribution of API particles over the carrier (attachment uniformity), to potentially proof the formation of agglomerates as well as to eventual changes between time points.

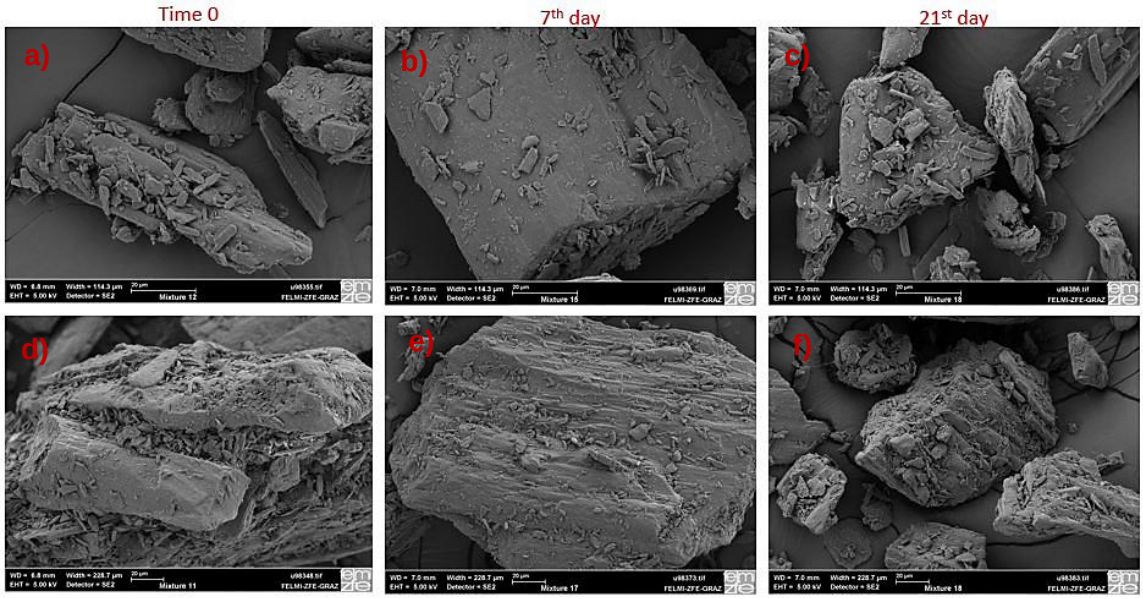

Figure 28: SEM images of mixtures containing milled SS a), b), c) with width 114.3µm; d), e) and f) with width 228.7µm

In general, SEM images of the mixtures containing jet-milled SS demonstrate that the API is well distributed over the carrier surface. However, it is visible that more API is attached with time as well as the presence of agglomerates increases.

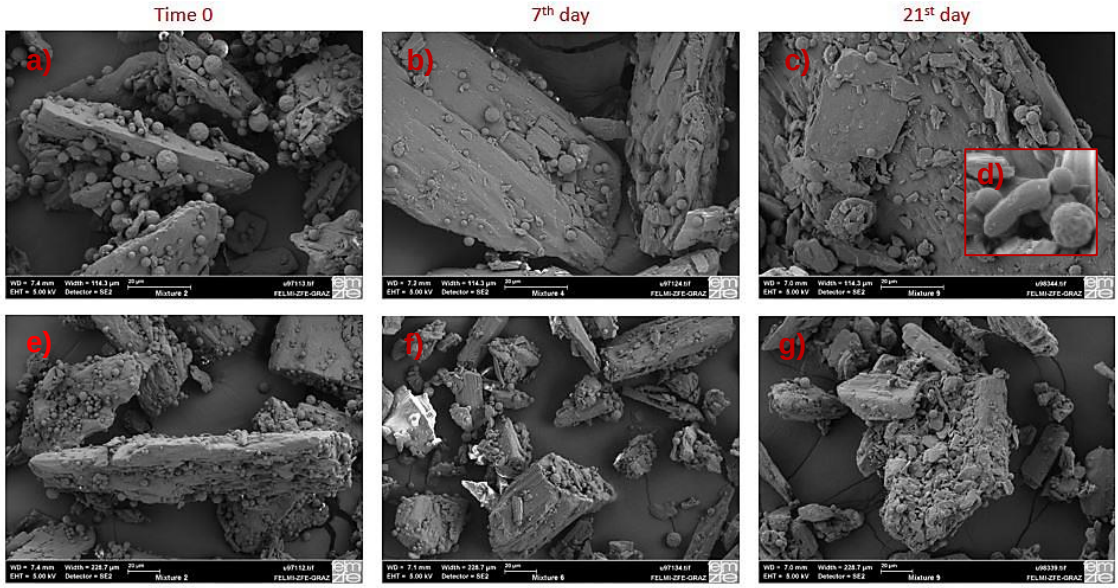

Figure 29: SEM images of mixtures containing spray dried SS a), b), c) with width 114.3µm; d) formation of the sinter bridge, e), f) and g) with width 228.7µm

SEM images of mixtures containing spray dried particles showed better distribution of the API particles on the carrier surface with time. Moreover, the formation of sinter bridge could be visualized on the SEM images, Figure 29 d). Moisture uptake onto the particles surface might promote surface dissolution and the formation of a bridge between neighboring particles.

3.2.3. Assessment of fine particles

Despite the bad mixing homogeneity, the aerodynamic performance of the different mixtures was analyzed. At this point, it has to be mentioned that results from these experiments have to be carefully interpreted and might be misleading. Nevertheless, to estimate an overall trend these tests were performed. The aerodynamic performance of the different mixtures at different time points was evaluated using the NGI. The NGI separates particles by its 8 stages with the cut-off diameters for stage 1 (St 1) 6.12µm, stage 2 (St 2) 3.42µm, stage 3 (St 3) 2.18µm, stage 4 (St 5) 1.31µm, stage 5 (St 5) 0.72µm, stage 6 (St 6) 0.40µm, stage 7 (St 7) 0.24µm and stage 8 (St 8) <0.24µm according to their aerodynamic diameter, when operating at flow rate of 100l/min. These values were calculated according to US Pharmacopeia [12].

Figures 30 and 31 illustrate the deposition of API particles from the DPI mixtures with jet-milled and spray dried SS, respectively, in the different stages of the impactor.

When considering the mass deposited in the inhaler mouth piece and throat, preseparator and different stages after aerosolization, the observations that have been made regarding the mixing homogeneity are reflected onto the aerosolization performance. Especially for mixtures containing the jet-milled API, the deviation in the deposited mass is quite high. In general, both mixtures showed not satisfactory performance, as a high percentage of the DPI mixture was deposited in the mouth piece, throat and preseparator. Therefore, both mixtures reflect poor API detachment behavior. Moreover, it was clearly observed during experiments, that in some cases, a significant amount of powder stayed in the capsules or the device.

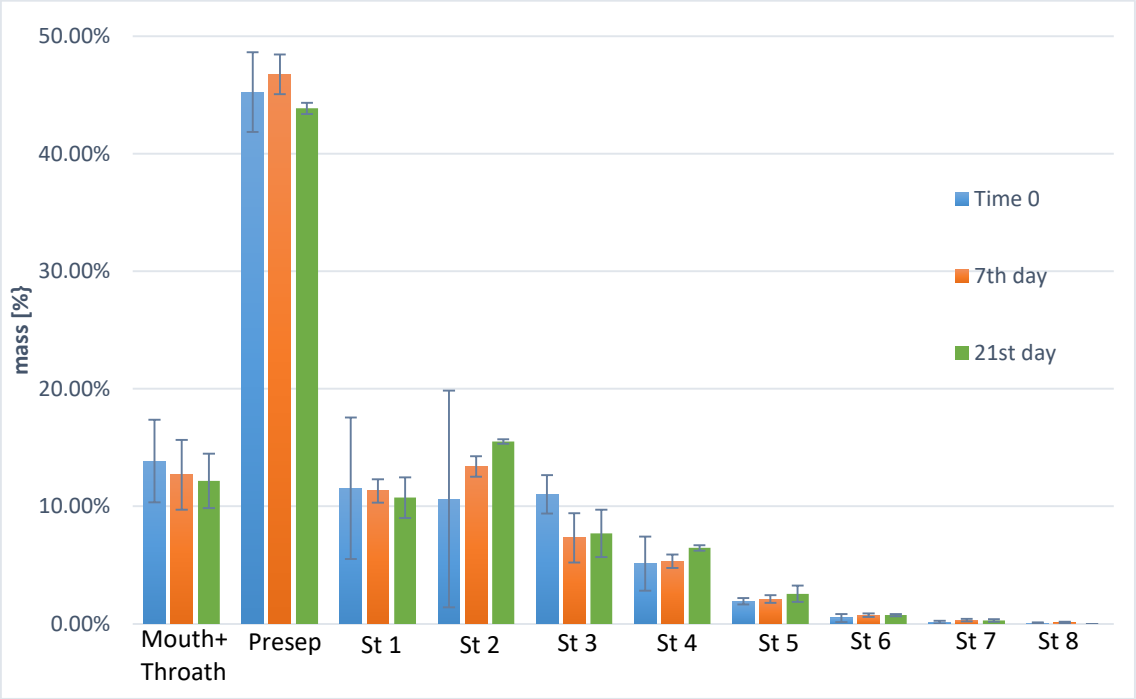

Figure 30: The amount of SS (% of mass) deposited on the inhaler mouth piece and throat, preseperator and different stages after aerosolization of the DPI mixtures containing milled SS (n=3 ± SD)

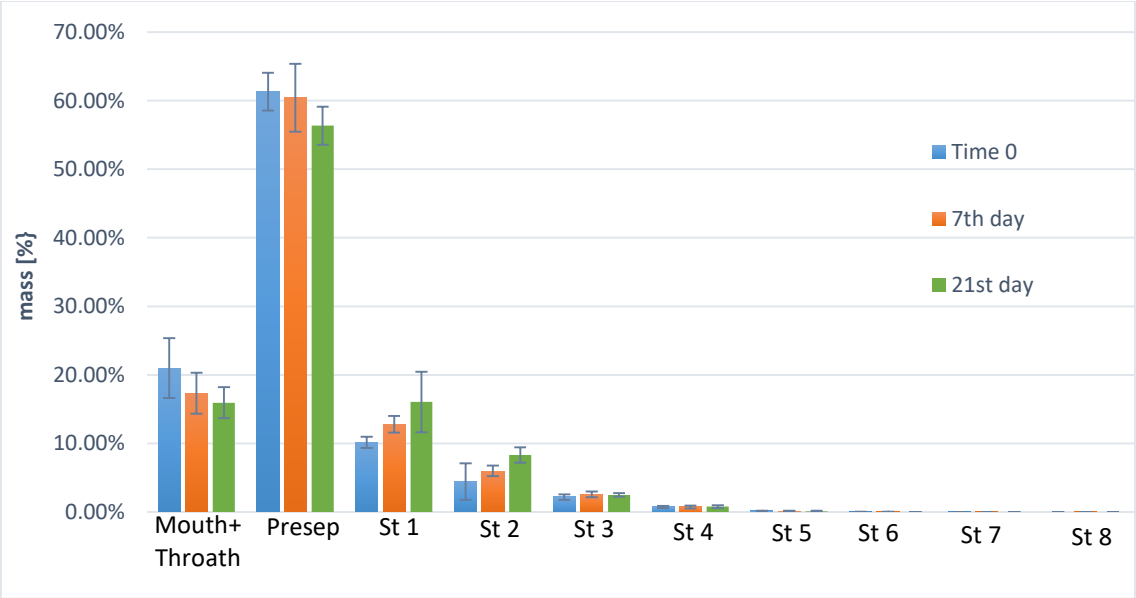

Figure 31: The amount of SS (% of mass) deposited on the inhaler mouth piece and throat, preseperator and different stages after aerosolization of the DPI mixtures containing spray dried SS (n=3 ± SD)

In order to be successfully deposited in the lung, the particle size of SS should be between 1-5μm. According to the cut-off diameter, that size corresponds to the stages 2-4. It can be seen that the amount of API deposited in this stages tendentially increased with time, especially for stage 2 and DPI formulation with jet-milled SS. As mentioned before, besides particle size, also the shape of the particles has an influence on the performance of DPI formulation. In our case, the superior performance of jet-milled API particles could be attributed to their shape. Needle-like shaped crystals have more ability to stay in the airflow than spherical shaped particles. Moreover, particles with more elongated shape will pack more loosely, reducing interparticulate forces. Consequently, carrier particles will exhibit lower adhesive forces with needle shaped elongated SS, leading to a better detachment which can be noted when comparing the emitted dose and the fine particle fraction (Figures 32 and 33).

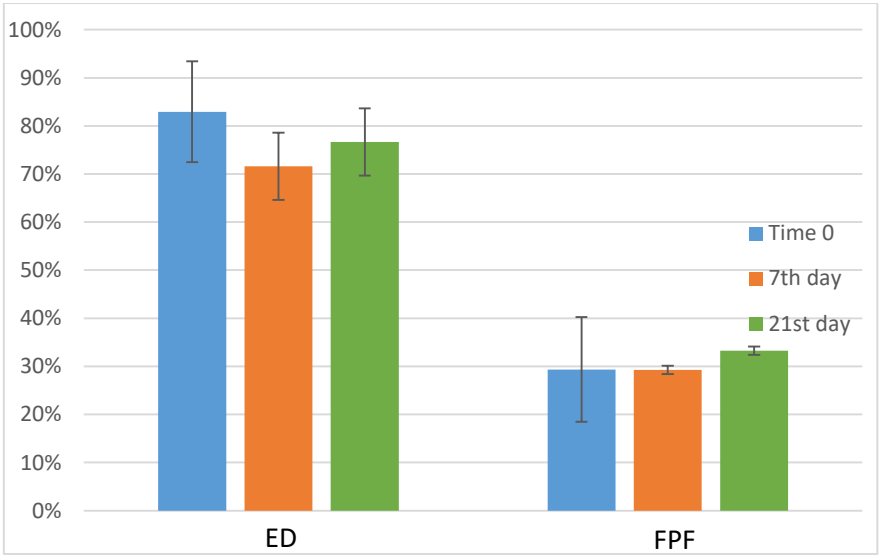

Figure 32: The comparison of ED [%] and FPF [%] for DPI formulation with milled SS

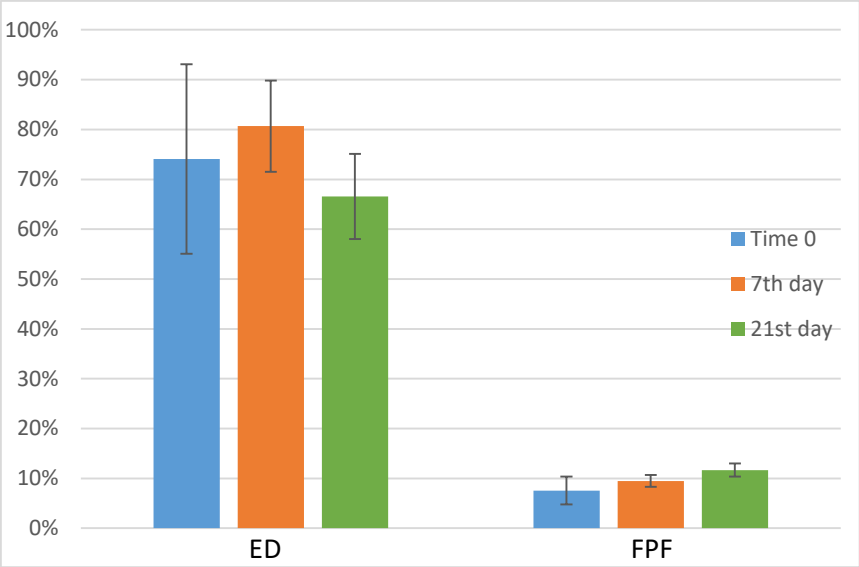

Figure 33: The comparison of ED [%] and FPF [%] for DPI formulation with spray dried SS

Both DPI formulations showed similar profiles regarding the emitted dose at time 0 and after 21 days. Taking the standard deviation into account the ED remained the same over time. Further, no significant differences concerning the ED between formulation comprising of spray dried or jet-milled API particles could be observed.

Regarding the FPF, overall jet-milled salbutamol sulphate led to higher FPFs (33%) than spray dried salbutamol (12%). Moreover, a slight increase over time could be observed for the spray dried as well as jet-milled API. The fact that the ED is about the same regardless of whether spray dried or jet-milled API is used and that the FPF is higher for jet-milled SS supports the hypothesis that drug detachment for the needle shape SS particles is favored. As discusses before, the formation of agglomerates was confirmed with SEM images, especially for the spray dried salbutamol particles. This phenomenon most likely affects the FPF. When these agglomerates do not break during inhalation they cannot reach the lung, resulting in relatively low FPF values.

Another explanaition for the improved performance of jet-milled salbutamol could be the smaller mean particle size distribution (x_{50}=1.23µm) of jet-milled particles compared to spray dried ones (x_{50}=3.88µm). However, surface free energy of the particles generated during the high impact milling process showed slight tendency towards higher values than spray dried particles. Usually one would

assume that milled particles have a higher surface free energy, resulting in higher adhesion and cohesion forces and thereby poorer aerosolization performance, which was not observed in the present study. The findings from the present study, in turn, are in agreement with findings reported by Cline and Dalby [61]. In their research, mixtures containing API with higher surface energy resulted in higher FPF and better detachment.

4. Conclusion and Outlook

The research performed within this thesis confirms that both processes investigated produced particles with appropriate size for deep lung penetration (1-5µm). Nevertheless, the different processing techniques significantly affect particle properties like shape and soli-state in contrasting ways. Optical microscopy analysis revealed that milled particles have a needle-like shape while spray dried particles are spherical. Regarding the solid-state of the generated API particles, FTIR analysis showed that jet-milled particles are predominantly crystalline whereas spray dried particles are mostly amorphous. This was additionally confirmed by SWAXS analysis. The performed DSC analysis showed that small amounts of amorphous fractions were generated during the milling process, which is in agreement with previous studies ([10, 37, 41, 62]). Furthermore, analysis of spray dried sample showed a substantial decrease of the glass temperature values under elevated humidity, indicating that amorphous sample might have absorbed high quantities of water which could have a substantial influence on the stability of the DPI formulation in the future.

The stability study revealed no changes in the solid-state of the particles with time (time 0, after 7, 14 and 21 days) or after storage under elevated humidity conditions (45% relative humidity). For the jet-milled particles also the shape did not change throughout the analysis and under elevated humidity conditions; the particles remained needle shaped. However, when stored under elevated humidity, the spray dried particles tend to change their shape from spherical to a more rod like shape over time. Moreover, after storage under increased humidity, in both samples the formation of sinter bridges was visible.

Aerodynamic assessment of both DPI formulations showed that higher FPFs were obtained when jet-milled salbutamol particles were used compared to spherical spray dried ones, which could be attributed to the needle-like shape of the API particles and the smaller particle size. The analysis of the ED between the different time points and both formulations resulted in similar profiles. This outcome of the aerodynamic assessment mainly could be the result of agglomeration formation and mixing conditions. Overall, a considerable amount of API was deposited in the mouth piece, throat and preseparator of the NGI device, especially for the spray dried material. This indicated insufficient drug detachment from the carrier most likely due to the formation of aggregates. The presence of the API agglomerates was confirmed via SEM images. Taking the standard deviation into account, the aerodynamic performance, meaning FPF and ED do not change over time.

Overall, future work should focus on water content analysis, in order to prevent recrystallization of the API particles as well as agglomeration formation. Moreover, the blending conditions have to be further investigated, to establish a mixing protocol that leads to a homogeneous API distribution within the blends. Additionally, the electrostatic charge of the particles should be investigated, as it can have a significant effect on the DPI performance [53]. These objectives will be another step towards better understanding of solid-state properties and its influence on the formulation stability and performance.

References

[1] N. R. Labiris, M. B. Dolovich, Pulmonary drug delivery. Part I: Physiological factors affecting therapeutic effectiveness of aerosolized medications, *J. Clin. Pharm.* 56 (2003) 588-599.

[2] W. Kaialya, G. P. Martin, H. Larhrib, M. D. Ticehurste, E. Kolosioneka., A. Nokhodchi, The influence of physical properties and morphology of crystallised lactose on delivery of salbutamol sulphate from dry powder inhalers, *Coll. and Surf. B: Biointerf. 89* (2012) 29-39.

[3] P. Colombo, D. Traini, F. Buttini, Inhalation drug delivery, 1st ed., John Wiley and Sons, UK, Europe (2013) 15-47, 91-116.

[4] X. M. Zeng, G. P. Martin, C. Marriott, Particulate Interactions in Dry Powder Formulations for Inhalation, Chapter 5, 1st ed., Taylor and Francis, UK, Europe (2001) 133-168.

[5] A.K. Mitra, D. Kwatra, A. D. Vadlapudi, Drug delivery, Chapter 5, 1st ed., Jones and Bartlett Learning, Massachusetts, USA, (2015) 71-108.

[6] K. Berkenfeld, A. Lamprecht, J. T. McConville, Devices for dry powder drug delivery to the lung, *AAPS Pharm. Sci. Tech.* 16 (2015) 479-490.

[7] P. J. Atkins, Dry Powder Inhalers: An overview, *Respiratory Care* 50 (2005) 1304-1312.

[8] http://emedicine.medscape.com/article/1413366-overview (10.08.2016)

[9] H. Yoshida, A. Kuwana, H. Shibata, K. Izutsu, Y. Goda, Comparison of aerodynamic particle size distribution between a Next Generation Impactor and a Cascade Impactor at a range of flow rates, *AAPS Pharm. Sci. Tech.* (2016) 1-8.

[10] A. H. L. Chow, H. H. Y. Tong, P. Chattopadhayay, B. Y. Shekunov, Particle engineering for pulmonary drug delivery, *Pharm. Res.* 24 (2007) 411-437.

[11] A. H. de Boer, D. Gjaltema, P. Hagedoorn, H. W. Frijlink, Characterization of inhalation aerosols: a critical evalution of cascade impactor analysis and laser diffraction technique, *Int. Jou. of Pharm.* 249 (2002) 219-231.

[12] U. S. Pharmacopeia, Chapter: Aerosols, nasal sprays, metered-dose inhalers and dry powder inhalers

[13] G. Buckton, Characterisation of small changes in the physical properties of powders of significance for dry powder inhaler formulations, *Adv. Drug Deliv. Rev.* 26 (1997) 17-27.

[14] X. Wu, X. Li, H. M. Mansour, Surface analytical techniques in solid-state particle characterization for predicting performance in dry powder inhalers, *Powder and Particle Jou.* 28 (2010) 3-19.

[15] L. Yu, Amorphous pharmaceutical solids: preparation, characterization and stabilization, *Adv. Drug Deliv. Rev.* 48 (2001) 27-42.

[16] R. Depasquale, S. L. Lee, J. Shur, R. Price, The influence of secondary processing on the structural relaxation dynamics of fluticasone propionate, AAPS Pharm. Sci. Tech, 16, (2015) 589-600.

[17] J. C. Freeley, P. York, B. S. Sumby, H. Dicks, Determination of surface properties and flow characteristics of salbutamol sulphate, before and after micronisation, *Int. Jou. of Pharm.* 172 (1998) 89-96.

[18] G. Buckton, P. Darcy, Assesment of disorder in crystalline powders – a review of analytical techniques and their application, *Int. Jou. of Pharm.* 179 (1999) 141-158.

[19] M. Rhodes, Introduction to particle technology, Chapter 1, 2nd ed., John Wiley and Sons, UK, Europe (2008) 1-29.

[20] T. Peng, S. Lin, B. Niu, X. Wang, Y. Huang, X. Zhang, G. Li, X. Pan, C. Wu, Influence of physical properties of carrier on the performance of dry powder inhalers, *Acta Pharm. Sin. B.* 6 (2016) 308-318.

[21] W. Kaialy, On the effects of blending, physicochemical properties and their interactions on the performance of carrier-based dry powders for inhalation – A review, *Adv. Colloid Interface Sci* (2016).

[22] W. Kaialy, M. N. Momin, M. D. Ticehurst, J. Murphy, A. Nokhodchi, Engineered mannitol as an alternative carrier to enhance deep lunge penetration

of salbutamol sulphate from dry powder inhaler, *Coll. and Surf. B: Biointerfaces* 79 (2010) 345-356.

[23] Y. Kawashima, T. Serigano, T. Hino, H. Yamamoto, H. Tekauchi, Effect of surface morphology of carrier lactose on dry powder inhalation property of pranlukast hydrate, *Int. Jou. of Pharm. 172* (1998) 179-188.

[24] M. J. Donovan, H. D. C. Smyth, Influence of size and surface roughness of large lactose carrier particles in dry powder inhaler formulations, *Int. Jou. of Pharm.* 402 (2010) 1-9.

[25] X. M. Zeng, K. H. Pandhal, G. P. Martin, The influence of lactose carrier on the content homogeneity and dispersibility of beclomethasone dipropionate from dry powder aerosols, *Int. Jou. of Pharm.* 197 (2000) 41-52.

[26] K. Stank, H. Steckel, Physico-chemical characterization of surface modified particles for inhalation, *Int. Jou. of Pharm.* 448 (2013) 9-18.

[27] T. Jong, J. Li, D. A. V. Morton, Q. Zhou, I. Larson, Investigation of the changes in aerosolization behavior between the jet-milled and spray-dried colistin ppowders through the surface energy characterization, *Jou. of Pharm. Sci.* (2016) 1-8.

[28] G. Buckton, H. Gill, The importance of surface energetics of powders for drug delivery and the establishment of inverse gas chromatography, , *Adv. Drug Deliv. Rev.* 59 (2007) 1474-1479.

[29] O. Planinšek, A. Trojak, S. Srčič, The dispersive component of the surface free energy of powders assessed using inverse gas chromatography and contact angle measurements, *Int. Jou. of Pharm.* 221 (2001) 211-217.

[30] J. T. Pinto, S. Zellnitz, M. Bresciani, J. G. Khinast, E. Roblegg, A. Paudel, Evaluation of the surface free energy of inhalable powders, *Drug Del. to the Lungs* 26 (2015)

[31] G. Bracco, B. Holst, Surface Science Techniques, Chapter 1, 1st ed., Springer Heidelberg, UK, Europe (2013) 3-29.

[32] S. Palzer, The effect of glass transition on the desired and undesired agglomeration of amorphous food powders, *Chem. Eng. Sci.* 60 (2005) 3959-3968.

[33] A. J. Hickey, H. M. Mansour, M. J. Telko, Z. Xu, H. D. C. Smyth, T. Mulder, R. Mclean, J. Langridge, D. Papadopoulos, Physical characterization of component particles included in dry powder inhalers. I: Strategy review and static characteristics, *Jou. of Pharm. Sci.* 96 (2007) 1282-1301.

[34] D. G. Bika, M. Gentzler, J. N. Michaels, Mechanical properties of agglomerates, *Powder Technology* 117 (2001) 98-112.

[35] S. Somiya, F. Aldinger, R. M. Spriggs, K. Uchino, K. Koumoto, M. Kaneno, Handbook of advanced ceramics, Chapter 4, 1st ed, Elsevier inc, UK, Europe, (2003) 187-265.

[36] S. R. B. Behara, P. Kippax, M. P. McIntosh, D. A. V. Morton, I. Larson, P. Stewart, Structural influence of cohesive mixtures of salbutamol sulphate and lactose on aerosolisation and de-agglomeration behaviour under dynamic conditions, *Eur. Jou. of Pharm. Sci.* 42 (2011) 210-219.

[37] G. Pilcer, K. Amighi, Formulation strategy and use of excipients in pulmonary drug delivery, *Int. Jou. of Pharm.* 392 (2010) 1-19.

[38] Buchi Nano Spray Dryer B-90 data sheet, (08.08.2016.) (http://static1.buchi.com/sites/default/files/technical-data-pdf/B 90_Data_Sheet_en_A_0.pdf?5ff8a47abe8e1d80fef6a5445b1a7a1fcafb0232)

[39] E. Faulhammer, V. Wahl, S. Zellnitz, J. G. Khinast, A. Paudel, Carrier-based dry powder inhalation: Impact of carrer modification on capsule filling processability and *in vitro* aerodynamic performance, *Int. Jou. of Pharm.* 491 (2015) 231-242.

[40] T. Müller, R. Krehl, J. Schiewe, C. Weiler, H. Steckel, Influence of small amorphous amounts in hydrophilic and hydrophobic APIs on storage stability of dry powder inhalation products, *Eur. Jou. of Pharm. and Biopharm.* 92 (2015) 130-138.

[41] K. Brodka-Pfeiffer, P. Langguth, P. Graß, H. Häusler, Influence on mechanical activation on the physical stability of salbutamol sulphate, *Eur. Jou. of Pharm. and Biopharm.* 56 (2003) 393-400.

[42] B. C. Hancock, G. Zografi, The relationship between the glass transition temperature and the water content of amorphous pharmaceutical solids, *Pharm. Res*. 11 (1994) 471-477.

[43] E. M. Littringer, Zellnitz S., Hammernik K., Adamer V., Friedl H., Urbanetz N. A., Spray drying of aqueous salbutamol sulphate solutions using the Nano Spray Dryer B-90-The impact of process parameters on particle size, *Drying Tech*. 31 (2013) 1346-1353.

[44] L. C. Grisedale, P. S. Belton, M. J. Jamieson, S. A. Barker, D. Q. M. Craig, An investigation into water interactions with amorphous and milled salbutamol sulphate: The development of predictive models for uptake and recrystallization, *Int. Jou. of Pharm.* 422 (2012) 220-228.

[45] S. Zellnitz, H. Schroettner, N. A. Urbanetz, Surface modified glass beads as model carriers in dry powder inhalers-Influence of drug load on the fine particle fraction, *Powder Tech.* 268 (2014) 377-386.

[46] Z. Z. Fang, Sintering of advanced materials-Fundamentals and Processed, Chapter 1, 1st ed, Woodhead Publishing, UK, Europe, (2010) 1-33.

[47] R. A. Storey, I. Ymen, Solid state characterization of pharmaceuticals, Chapter 2 and 4, 1st ed, John Wiley & Sons, UK, Europe (2011) 35-71, 135-187.

[48] H. R. H. Ali, H. G. M. Edwards, J. Kendrick, I. J. Scowen, Vibrational spectroscopic study of salbutamol hemisulphate, *Drug Test. Analysis* 1 (2009) 51-56.

[49] L. Tajber, D. O. Corrigan, O. I. Corrigan, A. M. Healy, Spray drying of budesonide, formoterol fumarate and their composites-I. Physicochemical characterization, *Int. Jou. of Pharm.* 376 (2009) 79-85.

[50] S. Zellnitz, O. Narygina, C. Resch, H. Schroettner, N. A. Urbanetz, Crystallization speed of salbutamol as a function of relative humidity and temperature, *Int. Jou. of Pharm.* 489 (2015) 150-176.

[51] M. Hartmann, S. Palzer, Caking of amorphous powders-material aspects, modelling and applications*, Powder Techn.* 206 (2011) 112-121.

[52] F. Podczeck, J. M. Newton, M. B. James, Influence of relative humidity of storage air on the adhesion and autoadhesion of micronized particles to particulate and compacted powder surfaces, *Jou. of Col. and Interf. Sci.* 187 (1997) 484-491.

[53] W. Kaialy, A review of factors affecting electrostatic charging of pharmaceuticals and adhesive mixtures for inhalation, Int. Jou. of Pharm. 503 (2016) 262-276.

[54] F. Sonvico, V. Coleman, D. Traini, P. M. Young, Evolved gas analysis during thermal degradation of salbutamol sulphate, *Jou. of Therm. Anal. Calorim.* 120 (2015) 789-794.

[55] C. J. Van Oss, R. F. Giese, W. Wu, On the predominant electron-donicity of polar solid surfaces, *The Jou. of Adh.* 63 (1997) 71-88.

[56] G. Bracco, B. Holst, Surface science techniques, Chapter 1, 1st ed., Springer-Verlag, Germany, Europe, 3-35.

[57] C. Sellitti, S. Vargiu, E. Martuscelli, D. Fabbro, Wettability of glass fibres with different sizings and their adhesion to unsaturated polyester matrices, *Jou. of Mat. Sci.* 22 (1987) 3477-3484.

[58] B. C. Hancock, M. Parks, What is the true solubility advantage for amorphous pharmaceuticals?, *Pharm. Res.* 17 (2000) 397-404.

[59] M. H. Shairare, M. de Matas, P. York, Effect of crystallization conditions and feedstock morphology on the aerosolization performance of micronized salbutamol sulphate, *Int. Jou. of Pharm.* 415 (2011) 62-72.

[60] S. R. B. Behara, I. Larson, P. Kippax, D. A. V. Morton, P. Stewart, An approach to characterizing the cohesive behavior of powders using a flow titration aerosolisation based methodology, *Chem. Eng. Sci. 66* (2011) 1640-1648.

[61] D. Cline and R. Dalby, Predicting the quality of powders for inhalation from surface energy and area, *Pharm. Res.* 19 (2002) 1274-1277.

[62] L. C. Grisedale, M. J. Jamieson, P. S. Belton, S. A. Barker, D. Q. M. Craig, Characterization and quantification of amorphous material in milled and spray dried salbutamol sulphate: a comparison of thermal, spectroscopic and water vapor sorption approaches, Jou. of Pharm. Sci. 100 (2011) 3114-3129.

List of tables

List of figures

List of abbreviations

API: Active Pharmaceutical Ingredient

MDIs: Metered Dose Inhalers

DPIs: Dry Powder Inhalers

APSD: Aerodynamic Particle Size Distribution

MMAD: Mass Median Aerodynamic Diameter

FPF: Fine Particle Fraction

d_A: Aerodynamic Diameter

ACI: Andersen Cascade Impactor

MSLI: Multi-Stage Liquid Impinger

NGI: Next Generation Impactor

SS: Salbutamol Sulphate

PSD: Particle Size Distribution

IGC: Inverse Gas Chromatography

AFM: Atomic Force Microscope

CAB: Cohesive Adhesive Balance

Tg: Glass Transition Temperature

SWAXS: Small and Wide Angle X-ray Scattering

FTIR: Fourier Transform Infrared Spectroscopy

DSC: Differential Scanning Calorimetry

HPLC: High Pressure Liquid Chromatography

SEM: Scanning Electron Microscopy

RH: Relative Humidity

FPD: Fine Particle Dose

ED: Emitted Dose